Magnetic Ordering in $Er_2Ti_2O_7$ and Elastic Softening in $Tb_2Ti_2O_7$

by

©Mona Alqarni

A thesis submitted to the School of Graduate Studies in partial fulfillment of the requirements for the degree of

Master of Science (Physics)

Department of Physics and Physical Oceanography
Memorial University of Newfoundland

Memorial University of Newfoundland

May 2016

ST. JOHN'S NEWFOUNDLAND

Abstract

Geometric frustration occurs in the rare earth pyrochlores due to magnetic rare earth ions occupying the vertices of the network of corner-sharing tetrahedra. In this research, we have two parts. In the first one we study the phase transition to the magnetically ordered state at low temperature in the pyrochlore $Er_2Ti_2O_7$. The molecular field method was used to solve this problem. In the second part, we analyse the crystal electric field Hamiltonian for the rare earth sites. The rather large degeneracy of the angular momentum J of the rare earth ion is lifted by the crystal electric field due to the neighboring ions in the crystal. By rewriting the Stevens operators in the crystal electric field Hamiltonian H_{CEF} in terms of charge quadruple operators, we can identify unstable order parameters in H_{CEF}. These may be related to lattice instabilities in $Tb_2Ti_2O_7$.

Acknowledgements

I would like first to thank my god who helped me to complete this thesis. Also, I would like to express my sincere gratitude to my supervisor, Dr. Stephanie Curnoe, whose understanding, patience and expertise added considerably to my graduate degree. Besides my supervisor, I would like to thank my parents, who were always supporting and encouraging me with their best wishes. I would like to thank my husband, Fawaz Alqarni, for his continuous support throughout my studies in Canada. Very special thanks goes out to the Saudi Bureau for their financial support throughout my degree.

Table of Contents

List of Tables

List of Figures

Chapter 1

Introduction

1.1 Rare earth pyrochlore

Pyrochlore crystals, which possess the general formula $A_2B_2O_7$, have an important type of structure known as geometrical frustration. The structure of the rare earth pyrochlore is cubic, and consists of A and B cations arranged in separate interpenetrating lattices of corner- sharing tetrahedra [1]. The A site is occupied by a rare earth element whose physical and chemical properties rely on its 4f electron shell occupation [1,2]. The rare earth pyrochlores show various physical characteristics, such as magnetic and thermodynamic properties, according to which rare earth ion is present and its magnetic moment [3, 4].

Over the past 15 years, the interaction between the nearest neighbors on the corner-sharing tetrahedral of the pyrochlores lattice has been of particular interest [3]. The nearest neighbor exchange interaction, along with long-range dipole-dipole interactions, are responsible for the spin liquid state in $Tb_2Ti_2O_7$ [5], magnetic ordering in $Er_2Ti_2O_7$ and the spin ice state in $Dy_2Ti_2O_7$ and $Ho_2Ti_2O_7$ [6,7].

1.2 Terbium titanate $Tb_2Ti_2O_7$

$Tb_2Ti_2O_7$ appears to be in a spin liquid state at low temperature [8]. A spin liquid is an unusual state that has short-range correlated spins but unbroken translation and rotation symmetry; these features can be observed in neutron scattering experiments [5]. In the last 15 years advanced theory and essential experiments on spin liquids have been achieved [8].

$Tb_2Ti_2O_7$ has unusual elastic properties. The earliest studies of $Tb_2Ti_2O_7$ found strong magnetostriction [9]. In a cubic system there are three elastic moduli -the bulk modulus C_{11} (associated with uniform volume changes), Young's modulus $(C_{11} - C_{12})$ (associated with volume preserving stretches along an axis) and the shear modulus C_{44}. In $Tb_2Ti_2O_7$, all three exhibit pronounced softening at low temperature indicative of a phase transition with an unknown order parameter [10].

Neutron-scattering studies are important methods for studying $Tb_2Ti_2O_7$. There are four important kinds of experiments using neutrons on $Tb_2Ti_2O_7$. The first one, neutron diffraction, along with x-ray absorption, was used to find the structure of $Tb_2Ti_2O_7$. $Tb_2Ti_2O_7$ was classified as pyrochlore crystal with space group $Fd\bar{3}m$ [11].

The crystal electric field (CEF) of $Tb_2Ti_2O_7$ is deduced by inelastic neutron-scattering [12]. The Tb^{3+} ions have a 13-fold degeneracy that is lifted by the crystal electric field. Inelastic neutron scattering can detect the difference in energy between CEF levels. The CEF Hamiltonian can be found by fits using these results. The ground state CEF level is a doublet, and so is the first excited state with an energy difference of approximately 18 K [8].

Diffuse neutron scattering is used to examine correlations in $Tb_2Ti_2O_7$. At 9 K, $Tb_2Ti_2O_7$ has short range correlations but no long range magnetic order [13]. Moreover, the ground state of $Tb_2Ti_2O_7$ is characterized by a large number of low energy

excitations but no long range order [8,14,15].

Finally, neutron spin echo is used to study the dynamics of the magnetic state of $Tb_2Ti_2O_7$. The magnetic state of $Tb_2Ti_2O_7$ appears to be freezing close to 200 mK, however the majority of spins have dynamic fluctuations down to below 50 mK [15].

1.3 Erbium titanate $Er_2Ti_2O_7$

$Er_2Ti_2O_7$ is distinctive because it is an antiferromagnetic pyrochlore that has been found to show planar anisotropy, with the local moments perpendicular to the [111] axes [6,16]. The magnetic order has been examined by neutron diffraction [16].

The properties of $Er_2Ti_2O_7$ at low temperature are well described by the anisotropic nearest neighbor exchange interaction [17]. But the mean field ground state of the model has continuous degeneracy. $Er_2Ti_2O_7$ is a rare example of a magnetic system that has an ordered ground state that is selected by quantum fluctuations. This phenomenon is called order-by-disorder (OBD) [18]. The experimental value of magnetic transition temperature for $Er_2Ti_2O_7$ equal to $1.2K$ [6].

1.4 Spin ice $Ho_2Ti_2O_7$ and $Dy_2Ti_2O_7$

The theory of spin ice has had great success in modern condensed matter physics [7]. In spin ice, the direction of the spins plays the same role as the location of the hydrogen ions in water ice [7]. Common water ice I_h is hexagonal and the space group is D^4_{6h}, with one oxygen atom and two hydrogen atoms in every molecule such that each oxygen atom has four neighboring hydrogen atoms [19]. In a water ice crystal, two hydrogen atoms are close to the oxygen atom (short bond), and the other two will be far the away (long bond) as shown in Figure 1.1. For this reason we have strong disorder of the hydrogen atoms and a periodic frame of oxygen atoms [20].

The two-close and two-far condition constrains the ground state of the crystal, which is highly degenerate with degeneracy Ω. The entropy, which is a quantitative measure of the amount of the thermal energy that unavailable to be useful, is $S = k_B \ln\Omega$ and the transition temperature is $1.8K$ [21,49].

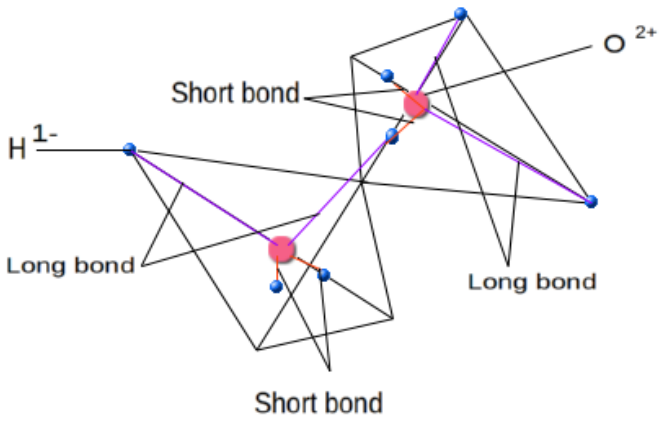

Figure 1.1: Water ice structure. Two oxygen ions are shown along with their neighboring hydrogen ions.

The ground state of the spin ice consists of two spins pointing into and two spins pointing out of each tetrahedron in the crystal, a ferromagnetic configuration as shown in Figure 1.2 [19]. Moreover, the thermodynamic properties depend on the calculation of the energy that includes the long range dipole-dipole interaction and the nearest-neighbour exchange interaction [7].

The spin ice state has two spins pointing in and two spins pointing out of each tetrahedron on the lattice. Each spin is located at a vertex that is shared by two tetrahedra. If we consider each spin dipole as two monopoles with opposite charge located in the centres of the two tetraheda then the net monopole is zero. However, if the dipole changes sign, then we will have three spins pointing out and one spin pointing in one tetrahedron, and vice versa on the other, so there will be a net positive

monopole on one tetrahedron, and a net negative monopole on the other. This has been observed as an electrically charged particle with one pole having net magnetic charge [19,22].

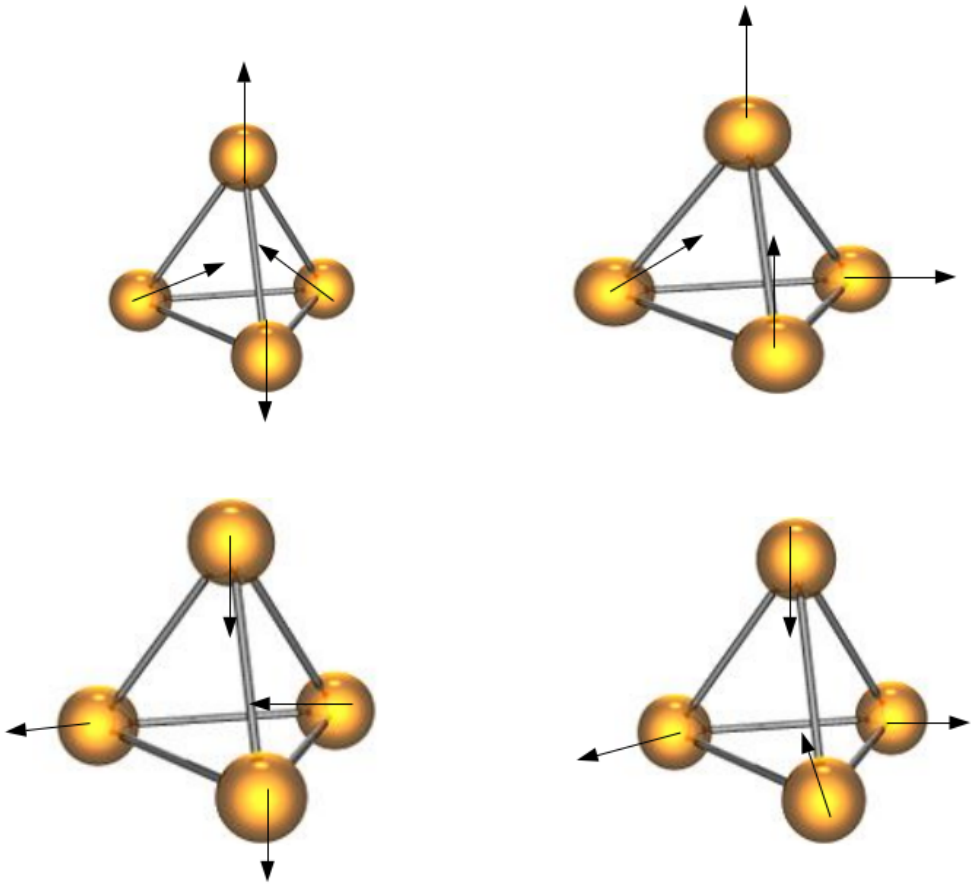

Figure 1.2: Four possible spin configurations of spin ice. Two spins point into and two spins point out of each tetrahedron.

	site	Coordinate position
Erbium/Terbium	16d	(0.5, 0.5, 0.5)
Titanium	16c	(0, 0, 0)
Oxygen	8b	$(0.375, 0.375, 0.375)$
Oxygen	48f	$(x, 0.125, 0.125)$

Table 1.1: Wyckoff positions of the ions in rare earth titanate pyrochlores.

1.5 Titanate pyrochlores $A_2Ti_2O_7$

1.5.1 Crystal structure of titanate pyrochlores

The pyrochlore compounds crystallize according to the chemical formula $A_2B_2O_7$ [23]. In this study we consider the rare earth titanate pyrochlores $Tb_2Ti_2O_7$ and $Er_2Ti_2O_7$. For these two compounds, the A-site is filled by the trivalent rare-earth ions with eight-fold oxygen coordination, terbium (Tb^{3+}) and erbium (Er^{3+}). The B-site is filled by Ti^{4+}, a tetravalent transition metal ion with six-fold oxygen coordination. The pyrochlores are face-centered cubic crystals belonging to the space group $Fd\bar{3}m$ (No. 227, O_h^7) with point group $m\bar{3}m$ (O_h). There are eight copies of the chemical formula $A_2B_2O_7$ per conventional unit cell. The A and B sites individually form infinite interpenetrating sublattices of corner-sharing tetrahedra, as shown in Figure 1.3 [8].

The Tb^{3+} and Er^{3+} ions occupy the 16d Wyckoff position (which will be discussed in the next subsection) located within a distorted cubic polyhedron with the coordinate position $(0.5, 0.5, 0.5)$, while the Ti^{4+} ions sit in the 16c Wyckoff position, and the oxygen ions occupy the 8b and 48f positions, as shown in Figure 1.3. The coordinates of each ion are given in Table 1.1 [24].

The bond lengths between the titanium and oxygen ions (Ti-O_{8b}) should be equal

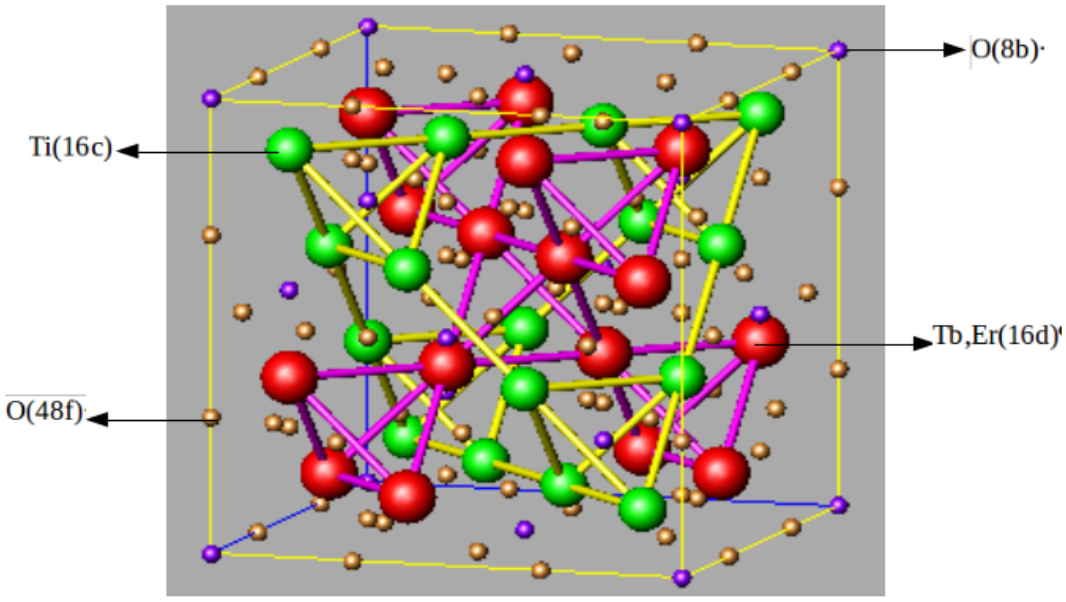

Figure 1.3: Conventional unit cell of a pyrochlore crystal, with the Wyckoff positions of each type of ion labelled. The rare earth (Tb /Er) and Ti^{4+} ions each form network of corner-sharing tetrahedra

and the angle between them will range between 130 and 135 degrees [8]. The length of the bond between the oxygen O_{48f} and the terbium or erbium ions is proportional to the x parameter (see Table 1.2) where x is the free position parameter allowed by the space group and depends on the material. There are many ways to determine the x parameter such as x-ray, electron and neutron diffraction, and theoretical simulations. The relationships between the A^{3+} ionic size for $Er_2Ti_2O_7$ and $Tb_2Ti_2O_7$ and the x free position parameter of oxygen ion, as well as the length of the bond between the oxygen and titanium ions, are shown in Table 1.2. Furthermore, to have a perfect cube, the parameter x must equal $\frac{3}{8}$. Therefore, the titanium site will be crystallized as a triangular octahedron and the Er or Tb site will be shaped like a regular cube [24].

Composition	A^{3+} ionic radius	O_{48f} x parameter	<A-O_{8b}>	<A-O_{48f}>	<Ti-O_{8b} >
$Tb_2Ti_2O_7$	1.04	0.3281(5)	2.199(1)	2.505(1)	1.963(2)
$Er_2Ti_2O_7$	1.004	0.3278(8)	2.182(1)	2.488(6)	1.946(3)

Table 1.2: Size and length parameters for $Tb_2Ti_2O_7$ and $Er_2Ti_2O_7$ (all lengths are in units of Å) [24].

1.5.2 Space group ($Fd\bar{3}m$)

The set of symmetry operations that leave a crystal invariant is called the space group [25]. As we mentioned in the previous chapter, $Er_2Ti_2O_7$ and $Tb_2Ti_2O_7$ crystallize with the space group $Fd\bar{3}m$ (O_h^7, No. 227). To examine the space group we should discuss some points according to the International Tables for Crystallography [26].

1.5.3 Hermann-Mauguin symbol

The short Hermann-Mauguin (HM) symbol $Fd\bar{3}m$ of the space group describes many properties of the pyrochlore crystal structure. Every letter and number in the HM symbol has a specific meaning:

(i)F: all face-centered. The lattice has four points per conventional unit cell with the coordinates $(0,0,0)$ $(0.5,0.5,0)$ $(0.5,0,0.5)$ $(0,0.5,0.5)$.

(ii) d: indicates a diamond glide plane.

(iii) $\bar{3}$: this number indicates that the space group has a 3-fold axis that contains an inversion point.

(iv) m: mirror plane (reflection plane).

The long symbol for this space group is $F4_1/d32/m$. Due to the normal and the axis symmetry which is parallel to the symmetry plane, we separate the symbol by the slash. In addition, there is a four-fold screw axis and right-hand screw rotation with vector $(\frac{1}{4})$t where t is the shortest translation of lattice which is parallel to the

axis in the same direction of the screw. Furthermore, the associated point group of this space group is O_h [26].

The space group $Fd\bar{3}m$ is non-symmorphic because it has screw rotations and glide reflections [26].

1.5.3.1 Origin choice

There are two origin choices for the space group $Fd\bar{3}m$:

(1) The origin is located at an inversion point, the 8a Wyckoff position.

(2) The origin is at the 16c Wyckoff position. This origin choice is used in this thesis.

If we would like to change the origin choice 1 to origin choice 2, we should add the vector $(-1/8, -1/8, -1/8)$ to the origin choice 1 to obtain origin choice 2 [26].

1.5.3.2 Wyckoff positions

Due to the information that is encoded in Wyckoff positions, they are an important part of the space group. Every point in the lattice has a site symmetry and a number of "equivalent point". When all of the point group symmetry operations are applied to a point in the crystal, those operations that leave the point invariant form the site symmetry group, while any new points that are generated are called "equivalent points" . Every point in the crystal is associated with a Wyckoff position, labelled by a number and a letter. The number is the number of equivalent points multiplied by the number of primitive cells contained in the conventional cell (for the fcc lattice, this number is 4). The letter is a simply a label for the Wyckoff position, beginning with a for the Wyckoff position with the highest site symmetry [26].

O_h	E	$8C_3$	$6C_2$	$6C_4$	$2C_2$	i	$6S_4$	$8S_6$	$3\sigma_h$	$6\sigma_d$
A_{1g}	1	1	1	1	1	1	1	1	1	1
A_{2g}	1	1	-1	-1	1	1	-1	1	1	-1
E_g	2	-1	0	0	2	2	0	-1	2	0
T_{1g}	3	0	-1	1	-1	3	1	0	-1	-1
T_{2g}	3	0	1	-1	-1	3	-1	0	-1	1
A_{1u}	1	1	1	1	1	-1	-1	-1	-1	-1
A_{2u}	1	1	-1	-1	1	-1	1	-1	-1	1
E_u	2	-1	0	0	2	-2	0	1	-2	0
T_{1u}	3	0	-1	1	-1	-3	-1	0	1	1
T_{2u}	3	0	1	-1	-1	-3	1	0	1	-1

Table 1.3: Character table of the point group O_h.

1.5.3.3 Irreducible representations

The character table contains useful information about a point group. The character table of O_h is shown in Table 2.1. The top row lists the set of symmetry operations of the point group grouped into classes. The first column lists the irreducible representations. The numbers are the character (trace) of the matrix representation of the symmetry operations [27].

Everything that is found in the O_h environment can be classified by the irreducible representations.

1.6 Other properties of $Er_2Ti_2O_7$ and $Tb_2Ti_2O_7$

In this section, we will discuss other properties of the titanate pyrochlores $A_2Ti_2O_7$ (A=Er, Tb). Due to the important role that the electronic configuration plays in determining the properties of these compounds, we will start with it for each element

	$Er_2Ti_2O_7$	$Tb_2Ti_2O_7$
density (g/cm^3)	7.039	6.662
A^{3+} ionic size (Å)	1.004	1.04
ion range (nm)	277.2	266.5
lattice parameter (Å)	10.0787	10.1589
$r_{\mathrm{Er,Tb}}$ / r_{Ti}	1.72	1.66

Table 1.4: Physical characteristics of $Er_2Ti_2O_7$ and $Tb_2Ti_2O_7$ [24].

in the compounds [25]. The electronic configuration is related to the atomic number according to the periodic table.

Erbium (Er^{3+}): $1s^2\ 2s^2\ 2p^6\ 3s^2\ 3p^6\ 3d^{10}\ 4s^2\ 4p^6\ 4d^{10}\ 5s^2\ 5p^6\ 4f^{12}\ 5d^0\ 6s^2$.

Terbium (Tb^{3+}): $1s^2\ 2s^2\ 2p^6\ 3s^2\ 3p^6\ 3d^{10}\ 4s^2\ 4p^6\ 4d^{10}\ 5s^2\ 5p^6\ 4f^9\ 5d^0\ 6s^2$.

Titanium (Ti^{4+}): $1s^2\ 2s^2\ 2p^6\ 3p^6\ 3d^2\ 4s^2$.

Oxygen (O^{2+}): $1s^2\ 2s^2\ 2p^4$.

Additional characteristics of the titanate pyrochlores are shown in Table 1.4. The electronic configuration and ionic radius (r) play an important role in the solid state chemistry of the titanate pyrochlores. When we have a look at the numbers of the lattice parameter of the compounds that were determined in 2003 by using the single crystal x-ray diffraction refinments and shown in Table 1.4, we find that they are in agreement with the results found in an earlier study by Subramanian *et al.* in 1983 [28].

1.7 Geometric frustration

The concept of frustration in physics refers to the situation where the system cannot satisfy all its magnetic exchange interactions at the same time. Because of the

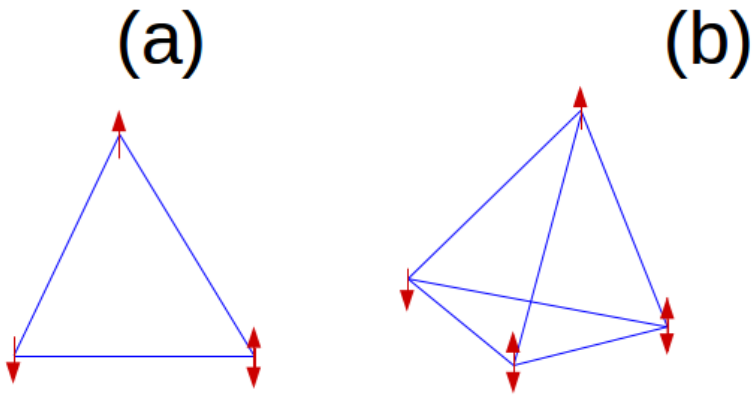

Figure 1.4: Geometric frustration: (a) on a triangle (b) on a tetrahedron. If the interaction is antiferromagnetic, then it is not possible for all of the spins to be oppositely aligned with each other.

competing interactions, the system is unable to find a unique ground state. Therefore, the ground state is degenerate in frustrated systems at low temperatures [29]. Competing interactions occur when, for example, the nearest neighbor interaction is ferromagnetic or anti-ferromagnetic and the next nearest neighbor interaction is anti-ferromagnet. Frustration also occur when magnetic ions are arranged in equilateral triangles and the interaction is anti-ferromagnetic. This is geometric frustration. Geometric frustration has been an intensively studied topic in the field of condensed matter physics. [30].

A clear model of two dimensional geometric frustration is the arrangement of three spins on the corners of an equilateral triangle, as shown in Figure 1.4a. The spins are constrained to point either up or down, and the energy is at minimum when each spin is aligned in the opposite direction as its neighbors. Another example is in three dimensions, when four identical spins are in the corners of a tetrahedron, as shown in Figure 1.4b [31].

In frustrated systems, triangles and tetrahedra can share either corners or edges

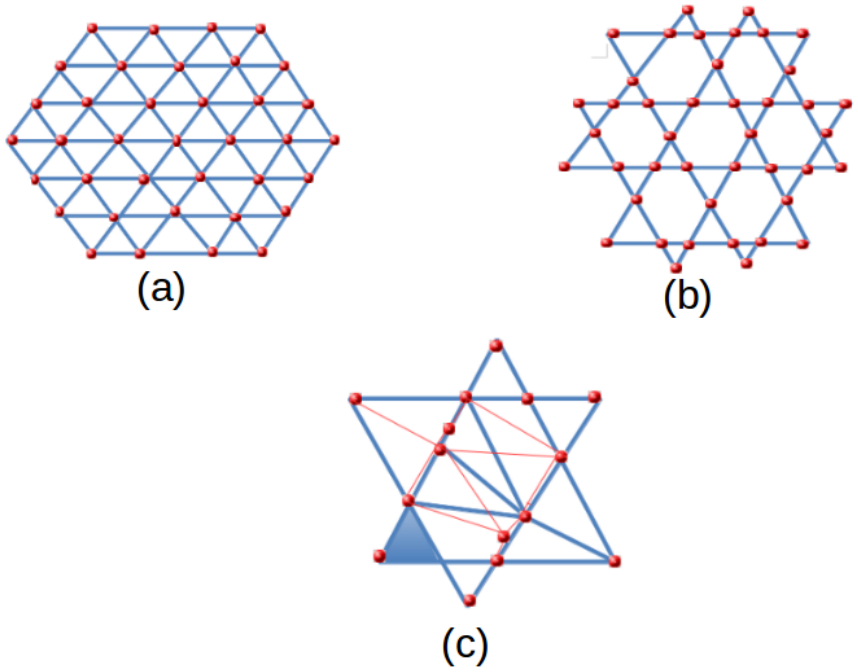

Figure 1.5: Geometrically frustrated lattices: (a) edge-sharing triangles; (b) corner-sharing triangles; (c) edge-sharing tetrahedra.

in the crystal lattice [28]. Therefore, there are four kinds of geometrically frustrated lattices, as shown in Figure 1.5 and Figure 1.3: edge-sharing triangles and tetrahedra are shown in Figure 1.5a and 1.5c, while the corner-sharing the triangles appear in Figure 1.5b and 1.3. The lattice shown in Figure 1.5b is called a kagome lattice. Figure 1.3 is the pyrochlore lattice. Figure 1.5c and Figure 1.3 show three dimensional crystals. The pyrochlore lattice is considered to be the most frustrated lattice because the corner-sharing tetrahedra in pyrochlore lattice show the clssical Heisenberg magnetic moments interacting with the nearest-neighbor antiferromagnetic coupling in which there is not transition to long-range magnetic order at finite temperature [30, 31].

1.8 Nearest neighbor exchange interaction on the pyrochlore lattice

Here we consider in a simple model Hamiltonian that describes the interaction between nearest neighbor (nn) spins,

$$H = -\mathcal{J} \sum_{<ij>} \vec{J}_i \cdot \vec{J}_j, \tag{1.1}$$

where $\mathcal{J}$ is the nn exchange interaction constant, <> represents the sum over pairs of nearest neighbors and $\vec{J}_i$ is the spin of the rare earth ion at the site i [32]. It is convenient to use a set of local axes, in which the local z axes of each rare earth ion points along the [111] directions [33]. We will use superscripts to indicate global axes, and subscripts to indicate local axes. J_i^α is the spin of i^{th} atom in the global $\alpha = x, y, z$ direction and $J_{i\alpha}$ is the spin of the i^{th} atom in the local coordinate system.

We will transform the Hamiltonian (1.1) in two steps. The first step is to change from global to local axes: this is so that the symmetry of the Hamiltonian is more evident. In the second step, we define magnetic order parameters, and write the Hamiltonian in terms of magnetic order parameters. We do this in order to analyse the Hamiltonian in context of Landau theory of phase transitions. In Landau theory, at a phase transition, only one of these order parameters becomes relevant (non-zero); the rest are not important.

The spin operators with respect to the local axes are:

for ion #1, at $(5/8, 5/8, 5/8)$;

$$J_{1x} = J_1^x\sqrt{6} + J_1^y\sqrt{6} - 2J_1^z\sqrt{6}, \tag{1.2}$$

$$J_{1y} = -J_1^x\sqrt{2} + J_1^y\sqrt{2}, \tag{1.3}$$

$$J_{1z} = J_1^x\sqrt{3} + J_1^y\sqrt{3} + J_1^z\sqrt{3}; \tag{1.4}$$

for ion #2, at $(3/8, 3/8, 5/8)$;

$$J_{2x} = J_2^x\sqrt{6} - J_2^y\sqrt{2} + J_2^z\sqrt{3}, \tag{1.5}$$

$$J_{2y} = -J_2^x\sqrt{2} - J_2^y\sqrt{2}, \tag{1.6}$$

$$J_{2z} = J_2^x\sqrt{3} - J_2^y\sqrt{3} + J_2^z\sqrt{3}; \tag{1.7}$$

for ion #3, at $(3/8, 5/8, 3/8)$;

$$J_{3x} = -J_3^x\sqrt{6} + J_3^y\sqrt{6} + 2J_3^z\sqrt{6}, \tag{1.8}$$

$$J_{3y} = -J_3^x\sqrt{2} + J_3^y\sqrt{2}, \tag{1.9}$$

$$J_{3z} = -J_3^x\sqrt{3} + J_3^y\sqrt{3} - J_3^z\sqrt{3}; \tag{1.10}$$

for ion #4, at $(5/8, 3/8, 3/8)$;

$$J_{4x} = -J_4^x\sqrt{6} - J_4^y\sqrt{6} + 2J_4^z\sqrt{6}, \tag{1.11}$$

$$J_{4y} = -J_4^x\sqrt{2} - J_4^y\sqrt{2}, \tag{1.12}$$

$$J_{4z} = J_4^x\sqrt{3} - J_4^y\sqrt{3} - J_4^z\sqrt{3}. \tag{1.13}$$

Equation (1.1) is the isotropic exchange interaction. However, in the pychrolore lattice, four different NN terms are allowed that are each invariant under the symmetry

operations of the pyrochlore space group [33]. We can write this as

$$H = \sum \mathcal{J}_1 X_1 + \mathcal{J}_2 X_2 + \mathcal{J}_3 X_3 + \mathcal{J}_4 X_4, \tag{1.14}$$

where the sum is over all tetrahedra and $\mathcal{J}_i$ are four independent coupling constants.[1] The exchange interactions X_i can be expressed in term of local coordinates of the Tb ions, as shown in Table 1.4. When $\mathcal{J}_1 = \mathcal{J}_2 = \mathcal{J}_3 = \mathcal{J}_4 = \mathcal{J}$, the interaction is isotropic, $\mathcal{J} \sum_{<ij>} \vec{J}_i \cdot \vec{J}_j$ [33].

In a single tetrahedron, there are four spins, therefore there are 12 spin components. It is convenient to group them into sums that transform according to the irredicible representations of O_h (the underlying point group of pyrochlore crystals).

[1] Although the use of the letter J for the coupling constant, and local and global spin operators may be confusing, it is standard [6,34,35,36,37],

Term	X_1	X_2	X_3
$\vec{J}_1 \cdot \vec{J}_2$	$-\frac{1}{3}J_{1z}J_{2z}$	$-\frac{\sqrt{2}}{3}[J_{1z}(J_{2+}+J_{2-})+(J_{1+}+J_{1-})J_{2z}]$	$\frac{1}{3}(J_{1+}J_{2+}+J_{1-}J_{2-})$
$\vec{J}_3 \cdot \vec{J}_4$	$-\frac{1}{3}J_{3z}J_{4z}$	$-\frac{\sqrt{2}}{3}[J_{3z}(J_{4+}+J_{4-})+(J_{3+}+J_{3-})J_{4z}]$	$\frac{1}{3}(J_{3+}J_{4+}+J_{3-}J_{4-})$
$\vec{J}_1 \cdot \vec{J}_3$	$-\frac{1}{3}J_{1z}J_{4z}$	$-\frac{\sqrt{2}}{3}[J_{1z}(J_{3+}+J_{3-})+(J_{1+}+J_{1-})J_{3z}]$	$\frac{1}{3}(\epsilon^2 J_{1+}J_{3+}+\epsilon J_{1-}J_{3-})$
$\vec{J}_2 \cdot \vec{J}_4$	$-\frac{1}{3}J_{2z}J_{4z}$	$-\frac{\sqrt{2}}{3}[J_{2z}(J_{4+}+J_{4-})+(J_{2+}+J_{2-})J_{4z}]$	$\frac{1}{3}(\epsilon^2 J_{2+}J_{4+}+\epsilon J_{2-}J_{4-})$
$\vec{J}_1 \cdot \vec{J}_4$	$-\frac{1}{3}J_{1z}J_{4z}$	$-\frac{\sqrt{2}}{3}[J_{1z}(J_{4+}+J_{4-})+(J_{1+}+J_{1-})J_{4z}]$	$\frac{1}{3}(\epsilon J_{1+}J_{4+}+\epsilon^2 J_{1-}J_{4-})$
$\vec{J}_2 \cdot \vec{J}_3$	$-\frac{1}{3}J_{2z}J_{3z}$	$-\frac{\sqrt{2}}{3}[J_{2z}(J_{3+}+J_{3-})+(J_{2+}+J_{2-})J_{3z}]$	$\frac{1}{3}(\epsilon J_{2+}J_{3+}+\epsilon^2 J_{2-}J_{3-})$

Term	X_4
$\vec{J}_1 \cdot \vec{J}_2$	$-\frac{1}{6}(J_{1+}J_{2-}+J_{1-}J_{2+})$
$\vec{J}_3 \cdot \vec{J}_4$	$-\frac{1}{6}(J_{3+}J_{4-}+J_{3-}J_{4+})$
$\vec{J}_1 \cdot \vec{J}_3$	$-\frac{1}{6}(J_{1+}J_{3-}+J_{1-}J_{3+})$
$\vec{J}_2 \cdot \vec{J}_4$	$-\frac{1}{6}(J_{2+}J_{4-}+J_{2-}J_{4+})$
$\vec{J}_1 \cdot \vec{J}_4$	$-\frac{1}{6}(J_{1+}J_{4-}+J_{1-}J_{4+})$
$\vec{J}_2 \cdot \vec{J}_3$	$-\frac{1}{6}(J_{2+}J_{3-}+J_{2-}J_{3+})$

Table 1.5: The exchange interaction for the pyrochlore lattice in terms of local coordinates. In each column, X_i is the sum of all the terms in the column. In each row, $\vec{J}_i \cdot \vec{J}_j$ is the sum of all the terms in the row [33]. $\epsilon = \exp 2\pi i/3$, and $J_\pm = J_x \pm iJ_y$.

$$J_{A_2} = J_{1z} + J_{2z} + J_{3z} + J_{4z}. \quad (1.15)$$

$$J_{T_{11x}} = J_{1z} - J_{2z} - J_{3z} + J_{4z}. \quad (1.16)$$

$$J_{T_{11y}} = J_{1z} - J_{2z} + J_{3z} - J_{4z}. \quad (1.17)$$

$$J_{T_{11z}} = J_{1z} + J_{2z} - J_{3z} - J_{4z}. \quad (1.18)$$

$$J_{E+} = J_{1+} + J_{2+} + J_{3+} + J_{4+}. \quad (1.19)$$

$$J_{E-} = J_{1-} + J_{2-} + J_{3-} + J_{4-}. \quad (1.20)$$

$$J_{T_{12x}} = \frac{1}{2}(\epsilon^2(J_{1+} - J_{2+} - J_{3+} + J_{4+}) + \epsilon(J_{1-} - J_{2-} - J_{3-} + J_{4-})). \quad (1.21)$$

$$J_{T_{12y}} = \frac{1}{2}(\epsilon(J_{1+} - J_{2+} + J_{3+} - J_{4+}) + \epsilon^2(J_{1-} - J_{2-} - J_{3-} + J_{4-}). \quad (1.22)$$

$$J_{T_{12z}} = J_{1x} + J_{2x} - J_{3x} - J_{4x}. \quad (1.23)$$

$$J_{T_{2x}} = \frac{i}{2}(-(\epsilon^2(J_{1+} - J_{2+} - J_{3+} + J_{4+}) + \epsilon(J_{1-} - J_{2-} - J_{3-} + J_{4-})). \quad (1.24)$$

$$J_{T_{2y}} = \frac{i}{2}(-\epsilon(J_{1+} - J_{2+} + J_{3+} - J_{4+}) + \epsilon^2(J_{1-} - J_{2-} + J_{3-} - J_{4-})). \quad (1.25)$$

$$J_{T_{2z}} = J_{1y} + J_{2y} - J_{3y} - J_{4y}, \quad (1.26)$$

where $\epsilon = \exp 2\pi i/3$, and $J_\pm = J_x \pm iJ_y$. In the above expressions, the subscripts on the left hand side are labels of the irreducible representations of the tetrahedral point group T_d: A_2 is a one-dimensional representation, E is a two-dimensional representation (the two different components are labelled as $\pm$) and T_1 and T_2 are three-dimensional representations (the three components are labelled by x, y, and z). There are actually two different sets of T_1 operators, called $J_{T_{1i}}$ and $J_{T_{1i}}$. In terms of these operators, the four exchange terms are:

$$X_1 = \frac{-1}{8}J_{A_2}^2 + \frac{1}{24}\vec{J}_{T_{1i}}^2 \quad (1.27)$$

$$X_2 = -\frac{\sqrt{2}}{3}\vec{J}_{T_{11}}.\vec{J}_{T_{12}} \tag{1.28}$$

$$X_3 = \frac{1}{6}\vec{J}^2_{T_{12}} - \frac{1}{6}\vec{J}^2_{T_2} \tag{1.29}$$

$$X_4 = -\frac{1}{8}J_{E_+}J_{E_-} + \frac{1}{24}\vec{J}^2_{T_{12}} + \frac{1}{24}\vec{J}^2_{T_2} \tag{1.30}$$

1.9 Motivation and Outline

This thesis explores possible order parameters $Er_2Ti_2O_7$and $Tb_2Ti_2O_7$ by examining instabilities orginating in the exchange Hamiltonian (for $Er_2Ti_2O_7$) and in the crystal electric field Hamiltonian ($Tb_2Ti_2O_7$).

In $Er_2Ti_2O_7$, the order parameter is known from neutron scattering studies [12] and the mechanism of the phase transition is known to be order-by-disorder [18]. Our calculations use the simplest approach, molecular field theory, to find an estimate of the ordering temperature beginning with the exchange Hamiltonian.

$Tb_2Ti_2O_7$ is a much bigger challenge. The observed elastic softening is a precursor to some kind of ordering phase transition, but no transition occurs. This thesis examines quadrupolar operators which appear inside the crystal electric field Hamiltonian for $Tb_2Ti_2O_7$ and $Er_2Ti_2O_7$. Mean field theory is used to identify possible quadrupolar order parameters in $Tb_2Ti_2O_7$.

In Chapter 2, the method of molecular field theory is reviewed. The crystal electric field Hamiltonian for the rare earth sites in a pyrochlore crystal is described.

In Chapter 3, we discuss magnetic ordering of $Er_2Ti_2O_7$. Using the exchange Hamiltonian as a starting point, we apply the molecular field method in order to calculate the critical temperature at which the magnetic operator $J_{E+} + J_{E-}$ becomes non-zero.

In Chapter 4, we examine the crystal electric field Hamiltonian for $Tb_2Ti_2O_7$

and $Er_2Ti_2O_7$. This calculation depends on re-writing H_{CEF} in terms of quadrupole operators, similar to the way the exchange interaction is written in terms of magnetic operators in the previous section.

Concluding remarks are made in Chapter 5.

Chapter 2

Methodology

2.1 Outline

In this chapter, we will take a closer look at the magnetic ordering of $Er_2Ti_2O_7$. After that, we will discuss molecular field theory, which will be applied to $Er_2Ti_2O_7$ in Chapter 3. Finally, we will consider the crystal electric field of rare earth pyrochlores.

2.2 Magnetic ordering of $Er_2Ti_2O_7$

$Er_2Ti_2O_7$ is an antiferromagnetic pyrochlore, where the magnetic moments are orthogonal to the local [111] symmetry axes, as discussed in Section 1.3. In addition, antiferromagnetic ordering occurs below the temperature T_N= 1.173 K with the propagation of wavevector $\vec{k}$=(0, 0, 0) [38]. This means that the magnetic structure is the same in every cell in every direction. The operators listed in Section 1.7 are possible magnetic order parameters for the rare earth pyrochlores. The magnetic structure of $Er_2Ti_2O_7$ corresponds to the order parameter $\psi_2 = J_{E_+} + J_{E_-}$, as shown in Figure 2.1 [6]. The arrows indicate the direction of magnetic moments in the ordered state. In Figure 2.1, each pair of spin is parallel [6]. The arrows indicate the direction of

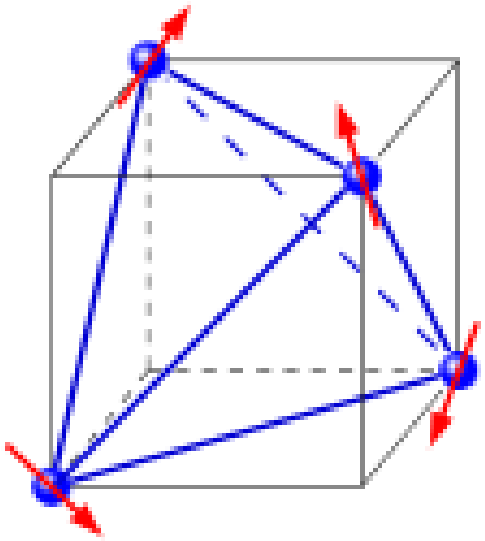

Figure 2.1: Antiferromagnetic order in $Er_2Ti_2O_7$.

magnetic moments in the order state. Magnetic ordering in $Er_2Ti_2O_7$ is detected by neutron scattering [39].

2.3 Molecular field approach

In a ferromagnet, below the critical temperature T_N, all the magnetic moments point in the same direction and the magnetization spontaneously happens, even if magnetic field is not applied. In an antiferromgnetic material, the magnetic moments are arranged to alternate between up and down, as shown in Figure 2.2 [40].

If we apply a magnetic field to the system, the Hamiltonian can be written in terms of the exchange energy due to the exchange interaction and the Zeeman energy,

$$H = -\mathcal{J} \sum_{<ij>} \vec{J_i} \cdot \vec{J_j} - g\mu_B \sum_j \vec{J_j} \cdot \vec{B}, \tag{2.1}$$

where $\mathcal{J}$ is the exchange constant which arises from the exchange between pairs of

nearest neighbours and $\vec{J}$ is the total angular momentum (spin) operator. Here the sum is over nearest neighbours (each pair of spins counted only once) [40,41]. We will replace the exchange interaction in Equation (2.1) by a molecular field B_{mf}. So it becomes,

$$H = -g\mu_B \sum_j \vec{J}_j \cdot (\vec{B} + \vec{B}_{mf}). \tag{2.2}$$

This is the Hamiltonian of a spin in a magnetic field $B + B_{mf}$, where the molecular field is

$$\vec{B}_{mf} = \frac{\mathcal{J} z}{g\mu_B} < \vec{J} > \tag{2.3}$$

where z is the number of nearest neighbors for each site and $< \vec{J} >$ is the thermal expectation value of the spin operator $\vec{J}$.

The molecular field is proportional to the spontaneous magnetization [42],

$$B_{mf} = \lambda M_s, \tag{2.4}$$

where λ is called the molecular field parameter [40,42].

We can express the spontaneous magnetization by :

$$M_s = ng\mu_B < J > \tag{2.5}$$

where n is the density of spins.

Using (2.3), (2.4) and (2.5), we find

$$\lambda = \frac{\mathcal{J} z}{ng^2\mu_B^2} \tag{2.6}$$

We now calculate the transition temperature T_N for a $J = 1/2$ (spin-1/2) system. To make it easier for calculations, we will assume that the spontaneous magnetisation

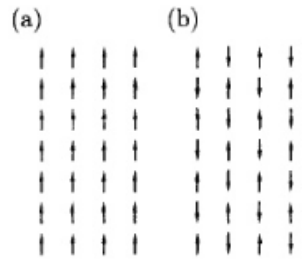

Figure 2.2: Spin arrangement in (a) ferromgnetism (b) antiferromgnetism.

occurs in the z-direction. Also note that all $\hbar$ are absorbed into the exchange constant $\mathcal{J}$, such that $\mathcal{J}$ has units of energy, and the value of the spin is $\pm\frac{1}{2}$.

We now calculate the transition temperature T_N. In the absence of an external field, the mean value of J_z on an arbitrary site is

$$< J_z >= \frac{\mathrm{Tr}\left[J_z e^{-H/k_B T}\right]}{Z_0} \tag{2.7}$$

where

$$H = g\mu_B J_z B_{mf} = -\mathcal{J} z J_z < J_z > \tag{2.8}$$

and

$$Z_0 = \mathrm{Tr}\left[e^{-H/k_B T}\right] = e^{-\frac{\mathcal{J}z<J_z>}{2k_B T}} + e^{\frac{\mathcal{J}z<J_z>}{2k_B T}}. \tag{2.9}$$

So, (2.7) becomes

$$<J_z> \;=\; \frac{1}{2}\left[\frac{e^{\frac{\mathcal{J}z<J_z>}{2k_B T}} - e^{-\frac{\mathcal{J}z<J_z>}{2k_B T}}}{e^{-\frac{\mathcal{J}z<J_z>}{2k_B T}} + e^{\frac{\mathcal{J}z<J_z>}{2k_B T}}}\right] \tag{2.10}$$

$$= \;\frac{1}{2}\tanh\frac{\mathcal{J}<J_z>}{2k_B T} \tag{2.11}$$

Just below the transition temperature, $< J_z >$ is small. By using the Taylor expansion

to represent the equation (2.11) becomes, for small $< J_z >$,

$$<J_z> = \left[\frac{\mathcal{J}<J_z>}{4k_BT}\right] \tag{2.12}$$

which allows us to solve for T_c

$$T_c = \frac{\mathcal{J}z}{4k_B}. \tag{2.13}$$

For a 1D chain, z =2. We will use a similar method to calculate T_c for the 1D spin $\frac{1}{2}$ antiferromagnet, and then for the antiferromagnetic pyrochlore $Er_2Ti_2O_7$.

2.3.1 1D spin $\frac{1}{2}$ antiferromagnet

While the 1D Ising model does not have a phase transition, we consider it to illustrate the mean field analogy.

2.3.1.1 Usual treatment

The Hamiltonian is

$$H = -\mathcal{J} \sum_{<ij>} \vec{J}_i \cdot \vec{J}_j. \tag{2.14}$$

Here $\mathcal{J}$ is a positive number and H is Heisenberg model. We are considering the expansion of (2.14) about some mean value. In this case, $< \vec{J}_j > = \pm \vec{J}$ where + is for oven numbered sites and - is for odd numbered sites. So we can write the Equation 2.14 as :

$$H = -2\mathcal{J} \sum_i \vec{J}_i (-1)^i \cdot <\vec{J}>. \tag{2.15}$$

The factor of 2 in the Equation (2.15) occurs because each site i has 2 nearest neighbours. Assuming $\vec{J}$ is a spin $\frac{1}{2}$ operator, the eigenvalues of Equation 2.15 are

$$E = \pm\mathcal{J} <| \vec{J} |> .$$

We assume that the spin will point in the z-direction, so $< \mid \vec{J} \mid >=< J_z >$. The mean value of the ith spin is

$$< J_{iz} >= \frac{\mathrm{Tr} < J_{iz} \exp(-H/k_B T_N) >}{Z_0}, \tag{2.16}$$

where

$$Z_0 = \exp \frac{-\mathcal{J} < J_z >}{k_B T} + \exp \frac{\mathcal{J} < J_z >}{k_B T}$$

When i is an even number,

$$\begin{aligned} <J_{iz}> &= \frac{1}{2} \left[\frac{e^{\frac{\mathcal{J}<J_z>}{2k_B T}} - e^{-\frac{\mathcal{J}<J_z>}{2k_B T}}}{e^{-\frac{\mathcal{J}<J_z>}{2k_B T}} + e^{\frac{\mathcal{J}<J_z>}{2k_B T}}} \right] & (2.17) \\ &= \frac{1}{2} \tanh \frac{\mathcal{J} < J_z >}{2k_B T} & (2.18) \end{aligned}$$

Now, we rewrite (2.18) by using Taylor expansion,

$$<J_{iz}> = \frac{1}{2} \left[\frac{\mathcal{J}<J_z>}{2k_B T_N} \right] \tag{2.19}$$

which gives the transition temperature as

$$T_N = \frac{\mathcal{J}}{2k_B}, \tag{2.20}$$

the same as 1D ferromagnet (section 2.13). When i is an odd number, the same transition temperature is found.

2.3.1.2 Group the spins

We will redo the spin $\frac{1}{2}$ antiferromagnetic chain by considering the spins in groups. This is the approach we will use for the more complicated problem of magnetic order

in $Er_2Ti_2O_7$. Furthermore, we now rename all the spins so that the spins are labelled as 1a, 1b, 2a, 2b, 3a, 3b, ...etc . The Hamiltonian is

$$H = \mathcal{J} \sum_i \vec{J}_{ia} \cdot \vec{J}_{ib} + \mathcal{J} \sum_i \vec{J}_{ib} \cdot \vec{J}_{(i+1)a}, \tag{2.21}$$

where $\mathcal{J}$ is a positive number. We define ferromagnetic and antiferromagnetic combinators of spins,

$$\vec{J}_i^F = \vec{J}_{ia} + \vec{J}_{ib} \tag{2.22}$$

$$\vec{J}_i^A = \vec{J}_{ia} - \vec{J}_{ib}. \tag{2.23}$$

From these equations we have

$$\vec{J}_{ia} = \left(\frac{\vec{J}_i^A + \vec{J}_i^F}{2} \right) \tag{2.24}$$

$$\vec{J}_{ib} = \left(\frac{-\vec{J}_i^A + \vec{J}_i^F}{2} \right) \tag{2.25}$$

which we substitute into H,

$$H = \mathcal{J} \sum_i \left(\frac{\vec{J}_i^A + \vec{J}_i^F}{2} \right) \left(\frac{-\vec{J}_i^A + \vec{J}_i^F}{2} \right) + \mathcal{J} \sum_i \left(\frac{\vec{J}_i^A + \vec{J}_i^F}{2} \right) \left(\frac{-\vec{J}_{i+1}^A + \vec{J}_{i+1}^F}{2} \right) \tag{2.26}$$

We assume that mean values of the spins in the z direction are

$$< J_{iz}^A >=< J >\neq 0 \tag{2.27}$$

and

$$< J_{iz}{}^F >= 0 \tag{2.28}$$

By using (2.27) and (2.28), the Equation (2.26) becomes

$$H_{MF} = -\mathcal{J}\sum_i J_{iz}^A < J > = \sum_i H_i \tag{2.29}$$

Where H_i is the molecular field Hamiltonian for the ith pair of spins. Assuming spin $\frac{1}{2}$ spins, the eigenstate of H_i are $| +- >$, $| -+ >$, $| ++ >$ and $| 00 >$ with eigenvalues $+\mathcal{J} < J >$, $-\mathcal{J} < J >$ and 0 (doubly degenerate), respectively. J_{iz}^A has the same eigenstates, with eigenvalues -1,1, and 0.

The mean value of ith pair of spins is,

$$\begin{aligned} < J_{iz}^A > &= < J > & (2.30)\\ &= \frac{\mathrm{Tr}\left[J_{iz}^A \exp^{-H/k_BT}\right]}{Z_0} & (2.31)\\ &= \frac{\left[e^{\frac{\mathcal{J}<J>}{k_BT}} - e^{-\frac{\mathcal{J}<J>}{k_BT}}\right]}{e^{-\frac{\mathcal{J}<J>}{k_BT}} + e^{\frac{\mathcal{J}<J>}{k_BT}} + 2} & (2.32) \end{aligned}$$

By using the Taylor expansion and (2.31), we have

$$< J >= \frac{2\mathcal{J} < J >}{4k_BT_N}$$

with a transition temperature.

$$T_N = \frac{1}{2}\frac{\mathcal{J}}{k_B},$$

as we obtained before. These results show us how to handle more complicated case involving groups of spins.

2.4 Crystal electric field Hamiltonian for the rare earth sites

The rare earths, which form a lattice of corner sharing tetrahedra, have various magnetic properties. In many cases, the crystal electric field (CEF) controls these magnetic properties partially [43], because of the significant interaction between the crystal electric field and 4f electron shell [44]. Eight oxygen ions surround each Tb ion, as described in Section 1.6.1, and these oxygen ions produce a local electric potential with symmetry D_{3d} [45].

In general, the crystal electric field Hamiltonian is :

$$H_{CEF} = \sum_{n=0,2,4...} \sum_{m=0}^{n} B_n^m O_n^m, \tag{2.33}$$

where B_n^m are the crystal field parameter constants whose values are obtained from inelastic neutron scattering experiments [44] and O_n^m are the Stevens equivalent operators that depend on J_z, J_+ and J_- [46]. n is the order of the polynomials of the operator $\vec{J}$ and m indexes operators with different symmetry.

For a crystal field with D_{3d} symmetry, the following Stevens operators appear in H_{CEF} [46]:

$$O_2^0 = 3J_z^2 - J(J+1) \tag{2.34}$$

$$O_4^0 = 35J_z^4 - 30J(J+1)J_z^2 + 25J_z^2 - 6J(J+1) + 3J^2(J+1)^2 \tag{2.35}$$

$$\begin{aligned} O_6^0 = {} & 231J_z^6 - 315J(J+1)J_z^4 + 735J_z^4 + 105J^2(J+1)^2J_z^2 - 525J(J+1)J_z^2 \\ & +294J_z^2 - 5J^3(J+1)^3 + 40J^2(J+1)^2 - 60J(J+1) \end{aligned} \tag{2.36}$$

$$O_4^3 = \{J_z, J_+^3 + J_-^3\}/4 \tag{2.37}$$

$$O_6^3 = \{J_z^3 - 3J_zJ(J+1) - 59J_z, J_+^3 + J_-^3\}/4 \tag{2.38}$$

$$O_6^6 = (J_+^6 + J_-^6)/2 \tag{2.39}$$

Therefore, we can reduce Equation 2.33 to

$$H_{CEF} = B_2^0O_2^0 + B_4^0O_4^0 + B_4^3O_4^3 + B_6^0O_6^0 + B_4^3O_6^3 + B_6^6O_6^6 \tag{2.40}$$

The crystal field parameters B_n^m can be determined using inelastic neutron scattering. The crystal field parameters for $Tb_2Ti_2O_7$ in (meV) are [44]

$$B_2^0 = -0.34 \tag{2.41}$$

$$B_4^0 = 4.9 \times 10^{-3} \tag{2.42}$$

$$B_4^3 = 4.3 \times 10^{-2} \tag{2.43}$$

$$B_6^0 = -7.9 \times 10^{-6} \tag{2.44}$$

$$B_4^3 = 1.30 \times 10^{-4} \tag{2.45}$$

$$B_6^6 = -1.08 \times 10^{-4} \tag{2.46}$$

The crystal field parameters for $Er_2Ti_2O_7$ in (meV) are [44]

$$B_2^0 = 7.5 \times 10^{-2} \tag{2.47}$$

$$B_4^0 = 1.41 \times 10^{-3} \tag{2.48}$$

$$B_4^3 = 1.25 \times 10^{-2} \tag{2.49}$$

$$B_6^0 = 1.09 \times 10^{-5} \tag{2.50}$$

$$B_4^3 = -1.8 \times 10^{-4} \tag{2.51}$$

$$B_6^6 = 1.5 \times 10^{-4}. \tag{2.52}$$

The crystal field parameter is determined by using

$$B_n^m = A_n^m < r^n > O_n \tag{2.53}$$

where A_n^m is the parameter which computed with the simple point charge ionic model,$< r^n >$ is the expectation value of the nth power distance between a nucleus and 4f electron shell and O_n is a Stevens parameter [44].

The eigenvalues of H_{CEF} are the energy levels sketched in Figure 2.3. The ground states for the $Tb_2Ti_2O_7$ and $Er_2Ti_2O_7$ are both doublets [44]. For $Tb_2Ti_2O_7$ ($J = 6$), we have

$$|\pm >= \pm 0.263|\pm 5 > -0.131|\mp 2 > \mp 0.128|\mp 1 > -0.97|\mp 4 >$$

and for $Er_2Ti_2O_7$ ($J = 15/2$), we have

$$|\pm >= .407|\pm 13/2 > \pm 0.390|\pm 7/2 > -0.558|\pm 1/2 > \mp 0.12|\pm 5/2 > +0.59|\mp 11/2 > .$$

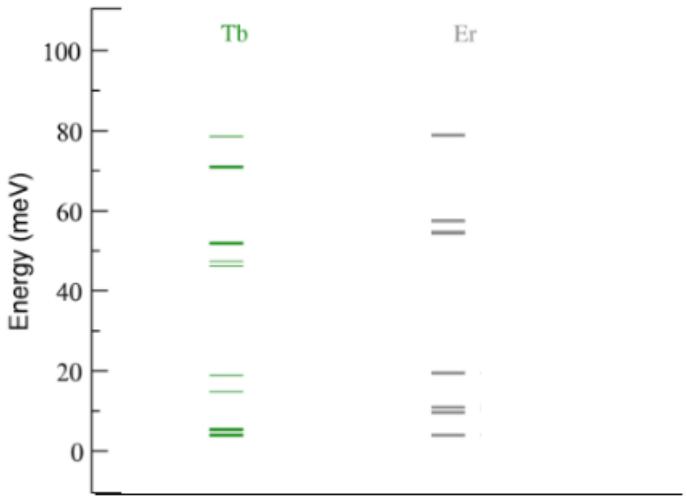

Figure 2.3: CEF energy levels of $Er_2Ti_2O_7$ and $Tb_2Ti_2O_7$. The thick lines are doublets and the thin lines are singlets [44].

Chapter 3

Magnetic Ordering of $Er_2Ti_2O_7$

3.1 Molecular field-method

In this chapter, we apply the methods of Chapter 2 to calculate the transition temperature for $Er_2Ti_2O_7$.

3.2 Calculation of the transition temperature (T_N) for $Er_2Ti_2O_7$

The exchange Hamiltonian (1.14) written in terms of the magnetic operators (1.27), (1.28), (1.29) and (1.30), is

$$H = \sum \mathcal{J}_1 \left[\frac{-1}{8} J_{A_2}^2 + \frac{1}{24} \vec{J}_{T_{11}}^2 \right] + \sum \mathcal{J}_2 \left[-\frac{\sqrt{2}}{3} \vec{J}_{T_{11}} . \vec{J}_{T_{12}} \right] +$$

$$\sum \mathcal{J}_3 \left[\frac{1}{6} \vec{J}_{T_{12}}^2 - \frac{1}{6} \vec{J}_{T_2}^2 \right] + \sum \mathcal{J}_4 \left[-\frac{1}{8} J_{E_+} J_{E_-} + \frac{1}{24} \vec{J}_{T_{12}}^2 + \frac{1}{24} \vec{J}_{T_2}^2 \right] \qquad (3.1)$$

where the sum is over all tetrahedra. The exchange constants for $Er_2Ti_2O_7$ have

been determined by fits to spin wave dispersion [34],

$$\mathcal{J}_1 = 0.075 \text{ meV} \tag{3.2}$$

$$\mathcal{J}_2 = -0.019 \text{ meV} \tag{3.3}$$

$$\mathcal{J}_3 = 0.126 \text{ meV} \tag{3.4}$$

$$\mathcal{J}_4 = 0.387 \text{ meV}. \tag{3.5}$$

To convert the exchange constant to kelvin, we need k_B where $k_B = \frac{1}{11600}$ eV/ K. So, the exchange constants in kelvin are

$$\mathcal{J}_1 = 0.87 \tag{3.6}$$

$$\mathcal{J}_2 = -0.22 \tag{3.7}$$

$$\mathcal{J}_3 = 1.46 \tag{3.8}$$

$$\mathcal{J}_4 = 4.5. \tag{3.9}$$

We have two types of tetrahedra (type A and type B), as shown in Figure 3.1. Therefore, the Hamiltonian for the entire tetrahedral network has two terms

$$H = H^A + H^B. \tag{3.10}$$

Furthermore, we have that

$$H^A = \sum_A \left(\mathcal{J}_1 X_1^A + \mathcal{J}_2 X_2^A + \mathcal{J}_3 X_3^A + \mathcal{J}_4 X_4^A \right) \tag{3.11}$$

where the sum is over all A tetrahedra. On the other hand, H^B is the exchange interaction over the set of B tetrahedra. H^B can be expressed in terms of A tetrahedra.

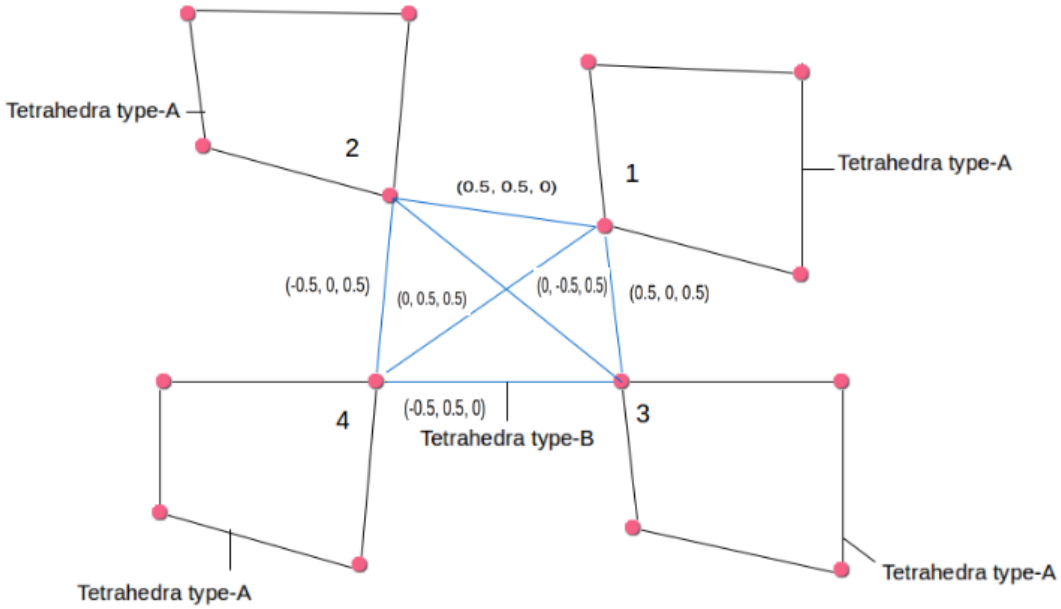

Figure 3.1: A and B tetrahedra inside the pyrochlore crystal.

All six of the exchange paths on a B tetrahedron can be written as interactions between sites that are on different A tetrahedra. Different A tetrahedra are related by the fcc lattice vectors, as shown in Figure 3.1.

For example, we can write

$$\sum_B X_1 = -\frac{1}{3}\sum_A \Big[J^A_{1z} J^{A+(\frac{1}{2},\frac{1}{2},0)}_{2z} + J^A_{1z} J^{A+(\frac{1}{2},0,\frac{1}{2})}_{3z} + J^A_{1z} J^{A+(0,\frac{1}{2},\frac{1}{2})}_{4z} + J^A_{2z} J^{A+(0,-\frac{1}{2},\frac{1}{2})}_{3z} + J^A_{2z} J^{A+(\frac{-1}{2},0,\frac{1}{2})}_{4z} + J^A_{3z} J^{A+(-\frac{1}{2},\frac{1}{2},0)}_{4z} \Big]. \tag{3.12}$$

This formulation is similar to the way we grouped pairs of spins in the previous section. In order to apply these methods we need to know the inverse relation for the magnetic

operators,

$$
\begin{aligned}
J_{1z} &= (J_{A_2} + J_{T_{11x}} + J_{T_{11y}} + J_{T_{11z}})/4 && (3.13)\\
J_{2z} &= (J_{A_2} - J_{T_{11x}} - J_{T_{11y}} + J_{T_{11z}})/4 && (3.14)\\
J_{3z} &= (J_{A_2} - J_{T_{11x}} + J_{T_{11y}} - J_{T_{11z}})/4 && (3.15)\\
J_{4z} &= (J_{A_2} + J_{T_{11x}} - J_{T_{11y}} - J_{T_{11z}})/4 && (3.16)\\
J_{1+} &= (J_{E-} + \epsilon J_{T_{12x}} + \epsilon^2 J_{T_{12y}} + J_{T_{12z}} + i\epsilon J_{T_{2x}} + i\epsilon^2 J_{T_{2y}} + iJ_{T_{2z}})/4 && (3.17)\\
J_{2+} &= (J_{E-} - \epsilon J_{T_{12x}} - \epsilon^2 J_{T_{12y}} + J_{T_{12z}} - i\epsilon J_{T_{2x}} - i\epsilon^2 J_{T_{2y}} + iJ_{T_{2z}})/4 && (3.18)\\
J_{3+} &= (J_{E-} - \epsilon J_{T_{12x}} + \epsilon^2 J_{T_{12y}} - J_{T_{12z}} - i\epsilon J_{T_{2x}} + i\epsilon^2 J_{T_{2y}} - iJ_{T_{2z}})/4 && (3.19)\\
J_{4+} &= (J_{E-} + \epsilon J_{T_{12x}} - \epsilon^2 J_{T_{12y}} - J_{T_{12z}} + i\epsilon J_{T_{2x}} - i\epsilon^2 J_{T_{2y}} - iJ_{T_{2z}})/4 && (3.20)\\
J_{1-} &= (J_{E+} + \epsilon^2 J_{T_{12x}} + \epsilon J_{T_{12y}} + J_{T_{12z}} - i\epsilon^2 J_{T_{2x}} - i\epsilon J_{T_{2y}} - iJ_{T_{2z}})/4 && (3.21)\\
J_{2-} &= (\vec{J}_{E+} - \epsilon^2 J_{T_{12x}} - \epsilon J_{T_{12y}} + J_{T_{12z}} + i\epsilon^2 J_{T_{2x}} + i\epsilon J_{T_{2y}} - iJ_{T_{2z}})/4 && (3.22)\\
J_{3-} &= (J_{E+} + \epsilon^2 J_{T_{12x}} - \epsilon J_{T_{12y}} - J_{T_{12z}} - i\epsilon^2 J_{T_{2x}} + i\epsilon J_{T_{2y}} + iJ_{T_{2z}})/4 && (3.23)
\end{aligned}
$$

where $i = \sqrt{-1}$ and $\epsilon = \exp 2\pi i/3$.

3.2.1 J_{A_2} order parameter

We begin by considering one component order parameter J_{A_2}. We assume that its mean value becomes non-zero at T_N, while the rest of the magnetic order parameters are zero because the order parameter J_{A_2} is uncoupled from the remaining degrees of freedom in the Hamiltonian. Therefore, it will be considered separately. So, we have

$$X_2 = 0$$

$$X_3 = 0$$

$$X_4 = 0$$

The Hamiltonian is

$$H = \mathcal{J}_1 \sum_{A,B} X_1 = -\frac{1}{8}\mathcal{J}_1 \sum_A J^A_{A_2} \cdot J^A_{A_2}$$

where we have assumed the second term that

$$< J_{T_{11}} > \;\; = \;\; 0. \tag{3.24}$$

so,

$$\sum_A X_1 = -\frac{1}{8} J^A_{A_2} \cdot J^A_{A_2} \tag{3.25}$$

and

$$\begin{aligned}
\sum_B X_1 &= -1/3 \sum_A \Big[J^A_{1z} J^{A+(\frac{1}{2},\frac{1}{2},0)}_{2z} + J^A_{1z} J^{A+(\frac{1}{2},0,\frac{1}{2})}_{3z} + J^A_{1z} J^{A+(0,\frac{1}{2},\frac{1}{2})}_{4z} + \\
&\quad J^A_{2z} J^{A+(0,-\frac{1}{2},\frac{1}{2})}_{3z} + J^A_{2z} J^{A+(\frac{1}{2},0,\frac{1}{2})}_{4z} + J^A_{3z} J^{A+(-\frac{1}{2},\frac{1}{2},0)}_{4z} \Big]. \\
&= -1/3 \sum_A \left[\frac{J^A_{A_2}}{4} \frac{J^{A+(\frac{1}{2},\frac{1}{2},0)}_{A_2}}{4} + \frac{J^A_{A_2}}{4} \frac{J^{A+(\frac{1}{2},0,\frac{1}{2})}_{A_2}}{4} + \frac{J^A_{1z} J^{A+(0,\frac{1}{2},\frac{1}{2})}_{4z}}{4} + \frac{J^A_{A_2}}{4} \frac{J^{A+(0,-\frac{1}{2},\frac{1}{2})}_{A_2}}{4} + \right. \\
&\quad \left. \frac{J^A_{A_2}}{4} \frac{J^{A+(\frac{-1}{2},0,\frac{1}{2})}_{A_2}}{4} + \frac{J^A_{A_2}}{4} \frac{J^{A+(-\frac{1}{2},\frac{1}{2},0)}_{A_2}}{4} \right].
\end{aligned}$$

Expanding around the mean value $< J_{A_2} >$, we have

$$\begin{aligned}
H &= \mathcal{J}_1 \left[-\frac{1}{8} \times 2 \sum_A J_{A_2} < J_{A_2} > -\frac{6}{3} \times \frac{2}{16} \sum_A J^A_{A_2} < J^A_{A_2} > \right] \\
&= -\frac{\mathcal{J}_1}{2} \sum_A J_{A_2} < J_{A_2} >
\end{aligned}$$

To calculate $< J_{A_2} >$, we will use the relation

$$
\begin{aligned}
< J_{A_2} > &= \frac{\mathrm{T}r[J_{A_2} e^{\frac{-H}{k_B T}}]}{Z_0} \\
&= \sum_S \frac{< S|J_{A_2} e^{-H/k_B T}|S >}{Z_0}
\end{aligned}
$$

where the states $|S>$ are the sixteen CEF ground states on a tetrahedron. With 4 sites on each tetrahedron, and two states $|\pm>$ per site, there are 16 states of the form

$$|S> = |\pm>_1 \otimes |\pm>_2 \otimes |\pm>_3 \otimes |\pm>_4 \equiv |\pm\pm\pm\pm>.$$

They are eigenstates of H with eigenvalues $-\frac{\mathcal{J}_1}{2} 2 < J_{A_2} > ij$, where i=4, 2, 0, -2, -4 and j is the matrix element for the CEF ground state, for Er^{3+} in $Er_2Ti_2O_7$,

$$j =< +|J_z|+ >= 0.75. \tag{3.26}$$

The eigenvalues with $i = \pm 4$ are non-degenerate, $i = \pm 2$ are 4-fold degenerate and $i = 0$ is 6-fold degenerate.

Z_0 is given by

$$
\begin{aligned}
Z_0 &= \sum_S < S|e^{-H/k_B T}|S > \\
&= e^{-\frac{\mathcal{J}_1}{2}\frac{<J_{A_2}>4j}{k_B T}} + 4e^{-\frac{\mathcal{J}_1}{2}\frac{<J_{A_2}>2j}{k_B T}} + 6 + \\
&\quad 4e^{\frac{\mathcal{J}_1}{2}\frac{<J_{A_2}>2j}{k_B T}} + e^{\frac{\mathcal{J}_1}{2}\frac{<J_{A_2}>2j}{k_B T}}
\end{aligned}
$$

and so

$$
\begin{aligned}
< J_{A_2} > &= j\left[\frac{4e^{\frac{\mathcal{J}_1}{2}\frac{<J_{A_2}>4j}{k_BT}} + 8e^{\frac{\mathcal{J}_1}{2}\frac{<J_{A_2}>2j}{k_BT}} - 8e^{\frac{-\mathcal{J}_1}{2}\frac{<J_{A_2}>2j}{k_BT}} - 4e^{\frac{-\mathcal{J}_1}{2}\frac{<J_{A_2}>4j}{k_BT}}}{Z_0}\right] \qquad (3.27)\\
&\approx \frac{j\left[4\frac{\mathcal{J}_1}{2}\frac{<J_{A_2}>4j}{k_BT} + 8\frac{\mathcal{J}_1}{2}\frac{<J_{A_2}>2j}{k_BT} + 8\frac{\mathcal{J}_1}{2}\frac{<J_{A_2}>2j}{k_BT} + 4\frac{\mathcal{J}_1}{2}\frac{<J_{A_2}>4j}{k_BT} + 8\frac{\mathcal{J}_1}{2}\frac{<J_{A_2}>2j}{k_BT}\right]}{16}\\
&= \frac{j^2 2\mathcal{J}_1 < J_{A_2} >}{k_BT}.
\end{aligned}
$$

This gives

$$
T_N = \frac{2j^2\mathcal{J}_1}{k_B}
$$

From the equations (3.6) and (3.26), we have

$$
\begin{aligned}
T_N &= \frac{2(0.75)^2(0.87)}{k_B}\\
&= 0.979 \text{ K} \qquad (3.28)
\end{aligned}
$$

3.2.2 J_E order parameter

We assume that the mean value of $J_{E_+} + J_{E_-}$ is not equal zero. This is the order parameter that actually occurs in $Er_2Ti_2O_7$. This phase has three different domains. If we rotate around the line that connects opposite corners of the unit cell by 120° (as shown in Figure 3.2), we will get $\epsilon J_{E_+} + \epsilon^2 J_{E_-}$, then if we rotate it again by 120°, we will have $\epsilon J_{E_-} + \epsilon^2 J_{E_+}$, where $\epsilon = \exp 2\pi i/3$.

We assume that the first domain appears with

$$
< J_{E+} + J_{E-} >=< J >
$$

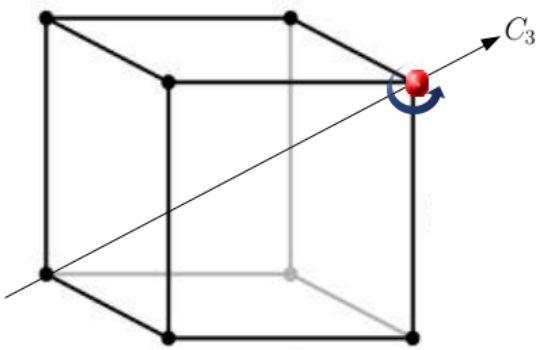

Figure 3.2: The rotation of the crystal by 120°. This a C_3 symmetry operation.

and

$$< J_{E+} - J_{E-} >= 0$$

which gives

$$< J_{E+} >=< J_{E-} >= \frac{< J >}{2} \tag{3.29}$$

We assume all other OP's (order parameter) vanish, therefore we only need to examine X_4 in H.

$$H = \mathcal{J}_4 \sum_{A,B} X_4 \tag{3.30}$$

The order parameter $< J_{E_+} + J_{E_-} >$ is uncoupled from the remaining degrees of freedom in the Hamiltonian, so we have assumed that $< J_{A_2} >$, $< \vec{J}_{T_1} >$ and $< \vec{J}_{T_2} >$ are zero.

So,

$$\sum_A X_4 \;\; = \;\; -1/8 \sum_A J^A_{E+} J^A_{E-}$$

and

$$\begin{aligned}
\sum_B X_4 &= -1/6 \sum_A \Big[J^A_{1+} J^{A+(\frac{1}{2},\frac{1}{2},0)}_{2-} + J^A_{1-} J^{A+(\frac{1}{2},\frac{1}{2},0)}_{2+} + J^A_{3+} J^{A+(-\frac{1}{2},\frac{1}{2},0)}_{4-} + J^A_{3-} J^{A+(\frac{1}{2},\frac{1}{2},0)}_{4+} \\
&\quad + J^A_{2-} J^{A+(0,\frac{1}{2},\frac{1}{2})}_{3+} + J^A_{2-} J^{A+(0,\frac{1}{2},\frac{1}{2})}_{3+} + J^A_{1+} J^{A+(\frac{1}{2},0,\frac{1}{2})}_{3-} + J^A_{1-} J^{A+(\frac{1}{2},0,\frac{1}{2})}_{3+} \\
&\quad + J^A_{2-} J^{A+(-\frac{1}{2},0,\frac{1}{2})}_{4+} + J^A_{2-} J^{A+(\frac{1}{2},0,\frac{1}{2})}_{4+} + J^A_{1+} J^{A+(0,-\frac{1}{2},\frac{1}{2})}_{4-} + J^A_{1-} J^{A+(0,-\frac{1}{2},\frac{1}{2})}_{4+} \Big] \\
&= -1/6 \sum_A \Big[\frac{J^A_{E-}}{4} \frac{J^{A+(\frac{1}{2},\frac{1}{2},0)}_{E+}}{4} + \frac{J^A_{E+}}{4} \frac{J^{A+(\frac{1}{2},\frac{1}{2},0)}_{E-}}{4} + \frac{J^A_{E-}}{4} \frac{J^{A+(-\frac{1}{2},\frac{1}{2},0)}_{E+}}{4} + \frac{J^A_{E+}}{4} \frac{J^{A+(-\frac{1}{2},\frac{1}{2},0)}_{E-}}{4} + \\
&\quad \frac{J^A_{E-}}{4} \frac{J^{A+(0,\frac{1}{2},\frac{1}{2})}_{E+}}{4} + \frac{J^A_{E+}}{4} \frac{J^{A+(0,\frac{1}{2},\frac{1}{2})}_{E-}}{4} + \frac{J^A_{E-}}{4} \frac{J^{A+(\frac{1}{2},0,\frac{1}{2})}_{E+}}{4} + \frac{J^A_{E+}}{4} \frac{J^{A+(\frac{1}{2},0,\frac{1}{2})}_{E-}}{4} + \\
&\quad \frac{J^A_{E-}}{4} \frac{J^{A+(-\frac{1}{2},0,\frac{1}{2})}_{E+}}{4} + \frac{J^A_{E+}}{4} \frac{J^{A+(-\frac{1}{2},0,\frac{1}{2})}_{E-}}{4} + \frac{J^A_{E-}}{4} \frac{J^{A+(0,-\frac{1}{2},\frac{1}{2})}_{E+}}{4} + \frac{J^A_{E+}}{4} \frac{J^{A+(0,-\frac{1}{2},\frac{1}{2})}_{E-}}{4} \Big]
\end{aligned}$$

Expanding around the mean value $< J_{E+} > = < J_{E-} > = < J >$, we have

$$\begin{aligned}
H &= \mathcal{J}_4 \Big[-\frac{1}{8} \sum_A \left(J^A_{E+} < J > + J^A_{E-} < J > \right) - \frac{1}{8} \sum_A \left(J^A_{E+} < J > + J^A_{E-} < J > \right) \Big] \\
&= -\frac{\mathcal{J}_4}{4} \sum_A \left(J^A_{E+} + J^A_{E-} \right) < J >
\end{aligned}$$

To calculate $< J^A_{E+} > = < J^A_{E-} > = < J >$, we use the relation

$$\begin{aligned}
< J_{E+} + J_{E-} > &= \frac{\mathrm{Tr} \left[\left(J_{E+} + J_{E-} \right) e^{-H/k_B T} \right]}{Z_0} \\
&= \frac{\sum\limits_S < S | \left(J_{E+} + J_{E-} \right) e^{-H/k_B T} | S >}{Z_0}
\end{aligned}$$

where $|S >$ are the 16 states on a tetrahedron. The eigenvalues of $J_{E+} + J_{E-} = 2(J_{1x} + J_{2x} + J_{3x} + J_{4x})$ are ti, where $i = 4, 2, 0, -2, -4$, with the degeneration 1, 4, 6, and 1 respectively, and t is the matrix element

$$t = < + | J_+ | - > = 6.42.$$

The eigenvalues of H are therefore $\frac{-\mathcal{J}_4}{4} < J > 2ti$. Then

$$\begin{aligned} Z_0 &= \sum_S < S|e^{-H/k_BT}|S > \qquad (3.31) \\ &= e^{\frac{-\mathcal{J}_4 < J > t}{k_BT}} + 4e^{\frac{-\mathcal{J}_4 < J > t}{2k_BT}} + 6 \\ &\quad +4e^{\frac{\mathcal{J}_4 < J > t}{2k_BT}} + e^{\frac{\mathcal{J}_4 < \ J > t}{k_BT}} \qquad (3.32) \end{aligned}$$

and

$$\begin{aligned} 2 < J > &= < J_{E+} + J_{E-} > \\ &= \frac{t}{Z_0}\left(4\exp\left[\frac{\mathcal{J}_4 < J > t}{k_BT}\right] + 4 \times 2\left[\exp\frac{\mathcal{J}_4 < J > t}{2k_BT}\right] + \right. \\ &\quad \left. -4 \times 2\exp\left[\frac{\mathcal{J}_4 < \vec{J} > t}{2k_BT_c}\right] - 4\left[\exp\frac{-\mathcal{J}_4 < J > t}{k_BT}\right]\right) \\ &\approx \frac{t\left[\frac{\mathcal{J}_4 < J > t}{k_BT} + \frac{4\mathcal{J}_4 < J > t}{k_BT} + \frac{4\mathcal{J}_4 < J > t}{k_BT} + \frac{\mathcal{J}_4 < J > t}{k_BT}\right]}{16} \\ &= \frac{t^2\mathcal{J}_4 < J >}{k_BT}. \qquad (3.33) \end{aligned}$$

This yields

$$\begin{aligned} 2 &= \frac{t^2\mathcal{J}_4}{k_BT_N} \\ 2k_BT_N &= (6.42)^2 4.5 \\ 2T_N &= (6.42)^2(4.5) \end{aligned}$$

so,

$$T_N = 93 \text{ K} \qquad (3.34)$$

3.3 Conclusion

Below T_N, the operator J_E has a non-zero expectation value and the magnitude of this operator$|\ J_{E+}^2 + J_{E-}^2\ |$ is considered in this calculation. However below T_N, the symmetry is not broken and magnetic ordering does not occur. In fact, the magnetic phase transition occurs at a much lower temperature by the order-by-disorder mechanism, where the order by disorder is a general phenomenon that does not have to occur in frustrated systems. Instead, T_N marks the appearance of a Goldstone mode- a gapless excitation associated with a continuous symmetry. For illustration, when we have a 2 component order parameter such as $\{J_{E+},J_{E-}\}$, we can draw the free energy as a function in 3D. It looks like a parabola above T_N (see Figure 3.3a), but below T_N the shape changes to a Mexican hat as shown in Figure 3.3b. In the parabola, the minimum of the free energy is at $|J_{E+}|^2+|J_{E-}|^2= 0$. In the Mexican hat, the minimum is a continuous circle for $|J_+|^2+|J_-|^2$ = constant. Since the minimum is anywhere on the circle, it costs no energy ("gapless") for the system to move from one point on the circle to another. This phenomenon occurs in many systems (see for example Ref.[47]).

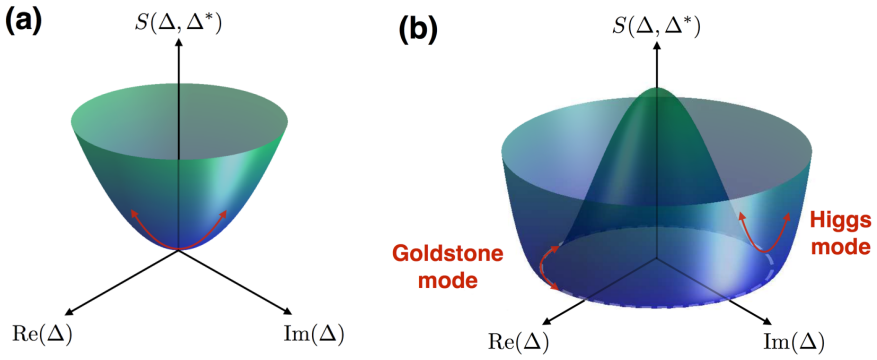

Figure 3.3: Function of the free energy for 2D order parameter. In this figure, Δ and Δ^* stand for J_{E+} and J_{E-}.

In order for symmetry breaking to occur, the free energy must contain a term

that creates local minima in the Mexican hat potential, such a term can be generated by the order-by -disorder mechchanism [6].

Chapter 4

Quadrupole instabilities in the crystal electric field Hamilton of $Tb_2Ti_2O_7$

4.1 Elastic properties of $Tb_2Ti_2O_7$

The experimental investigation of exotic elastic properties of $Tb_2Ti_2O_7$ at low temperature was carried out over twenty years ago [48]. The most striking feature is that all of the elastic modulii for this compound become soft at low temperature [10], as shown in Figure 4.1. This behaviour is normally the precursor to a phase transition, however no phase transition occurs even at the lowest temperatures. In this Chapter, we investigate possible quadrupolar order parameters hidden in the crystal electric field Hamiltonian.

The crystal electric field ground state and first excited states of the Tb^{3+} ions in $Tb_2Ti_2O_7$ can be estimated from the quadrupole susceptibility that is deduced from ultrasonic measurements. The CEF states can then be used to find (at least

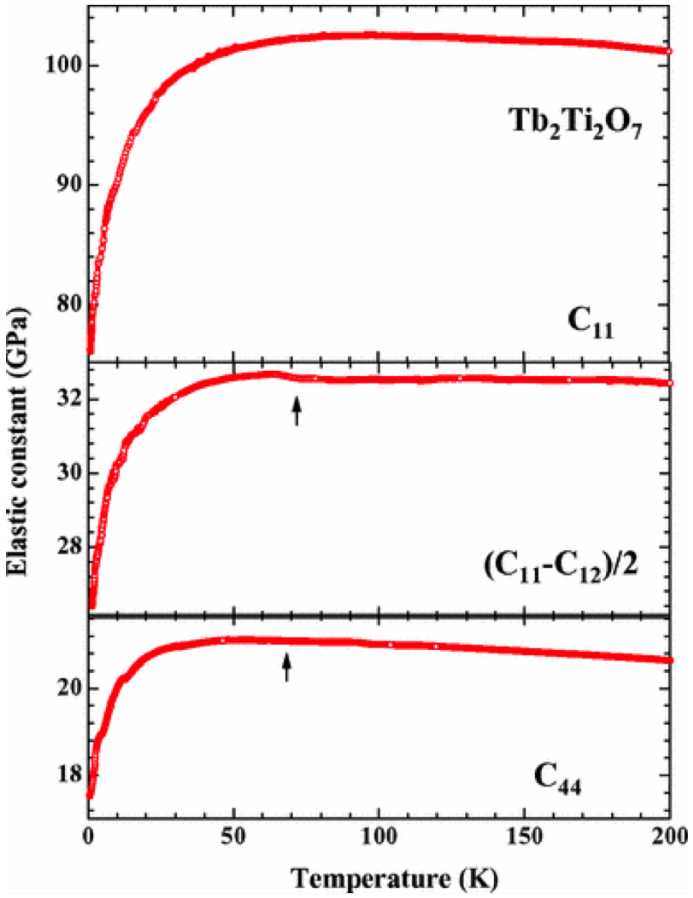

Figure 4.1: Temperaure dependece of elastic constant of $Tb_2Ti_2O_7$ where the arrow indicates to the anomaly [10].

approximately) the crystal electric field Hamiltonian, as was done many years ago [48].

Softening of the elastic constants can be attributed to linear coupling between elastic strain and some kind of order parameter. In order for the coupling to be linear the OP necessarily has the same symmetry as the strain. This rules out a magnetic phase transition because magnetic order parameters break time-reversal symmetry, while strains do not. Quadrupolar order parameters can match the symmetry of elastic strains. Here “quadrupolar" refers to electronic structure associated with the rare earth f-electrons[10].

Essentially, the free energy that includes elastic and some unknown OP looks like this:

$$F = C_{ij}e_ie_j + be_i\eta_i + a\eta_i^2 \tag{4.1}$$

where e_i is the strain tensor component and η_i is the order parameter, for $i = 1, \ldots 6$. The first term is the elastic term, which for cubic systems contains three parts (A_{1g} (dilatational), E_g (deviatoric) and T_{2g} (shear) strains), for a total of 6 strains e_i with three different elastic constants. The third term contains the OP, η_i in our case, one of the many quadrupolar OP's we will find. The second term couples the strain and the OP. The strain and the OP must have the same symmetry to be coupled in this way, so onlyA_{1g}, E_g and T_{2g} type OP's can couple to the strains. The constant a is proportional to $T - T_N$. If $a < 0$ then the free energy has a minimum for η_i non-zero where a depend on temperature. The elastic constants have a negative divergence (softening) when this happens. So the behaviour of the elastic constants can indicate if an order parameter is present

4.2 Stevens equivalent operators

In Section (2.4), we showed that all the Stevens equivalent operators are expressed in terms of $J_\pm$ and J_z. On the other hand, every quadrupole operator also has an expression in terms of $J_\pm$ and J_z. There are 24 different same-site quadrupolar operators (24 different operators of the form $J_k^i\ J_l^i$ where i is the site number and k, l are x, y, z). These 24 operators can be classified according to the irreducible representations of the point group. We find that complete set of same-site quadrapole

operators is

$$
\begin{aligned}
Q_{A_{11}} &= J_{1z}^2 + J_{2z}^2 + J_{3z}^2 + J_{4z}^2 && (4.2)\\
Q_{T_{21}^x} &= J_{1z}^2 - J_{2z}^2 - J_{3z}^2 + J_{4z}^2 && (4.3)\\
Q_{T_{21}^y} &= J_{1z}^2 - J_{2z}^2 + J_{3z}^2 - J_{4z}^2 && (4.4)\\
Q_{T_{21}^z} &= J_{1z}^2 + J_{2z}^2 - J_{3z}^2 - J_{4z}^2 && (4.5)\\
Q_{E+1} &= [\{J_{1z}, J_{1-}\} + \{J_{2z}, J_{2-}\} + \{J_{3z}, J_{3-}\} + \{J_{4z}, J_{4-}\}]/2 && (4.6)\\
Q_{E-1} &= [\{J_{1z}, J_{1+}\} + \{J_{2z}, J_{2+}\} + \{J_{3z}, J_{3+}\} + \{J_{4z}, J_{4+}\}]/2 && (4.7)\\
Q_{T_{11}^x} &= \{J_{1z}, -\sqrt{3}J_{1x}/2 - J_{1y}/2\} - \{J_{2z}, -\sqrt{3}J_{2x}/2 - J_{2y}/2\} - \\
&\quad \{J_{3z}, -\sqrt{3}J_{3x}/2 - J_{3y}/2\} - \{J_{4z}, -\sqrt{3}J_{4x}/2 - J_{4y}/2\} && (4.8)\\
Q_{T_{11}^y} &= \{J_{1z} - \sqrt{3}J_{1x}/2 - J_{1y}/2\} - \{J_{2z} - \sqrt{3}J_{2x}/2 - J_{2y}/2\} + \\
&\quad \{J_{3z}, -\sqrt{3}J_{3x}/2 - J_{3y}/2\} - \{J_{4z}, -\sqrt{3}J_{4x}/2 - J_{4y}/2\} && (4.9)\\
Q_{T_{11}^z} &= \{J_{1z}, J_{1y}\} + \{J_{2z}, J_{2y}\} - \{J_{3z}, J_{3y}\} - \{J_{4z}, J_{4y}\} && (4.10)\\
Q_{T_{22}^x} &= \{J_{1z}, +\sqrt{3}J_{1y}/2 - J_{1x}/2\} - \{J_{2z}, +\sqrt{3}J_{2y}/2 - J_{2x}/2\} + \\
&\quad \{J_{3z}, +\sqrt{3}J_{3y}/2 - J_{3x}/2\} - \{J_{4z}, +\sqrt{3}J_{4y}/2 - J_{4x}/2\} && (4.11)\\
Q_{T_{22}^y} &= \{J_{1z}, -\sqrt{3}J_{1y}/2 - J_{1x}/2\} - \{J_{2z}, -\sqrt{3}J_{2y}/2 - J_{2x}/2\} + \\
&\quad \{J_{3z}, -\sqrt{3}J_{3y}/2 - J_{3x}/2\} - \{J_{4z}, -\sqrt{3}J_{4y}/2 - J_{4x}/2\} && (4.12)\\
Q_{T_{22}^z} &= \{J_{1z}, J_{1x}\} + \{J_{2z}, J_{2x}\} - \{J_{3z}, J_{3x}\} - \{J_{4z}, J_{4x}\} && (4.13)\\
Q_{E+2} &= J_{1+}^2 + J_{2+}^2 + J_{3+}^2 + J_{4+}^2 && (4.14)\\
Q_{E-2} &= J_{1-}^2 + J_{2-}^2 + J_{3-}^2 + J_{4-}^2 && (4.15)\\
Q_{T_{23}^x} &= \epsilon J_{1+}^2 + \epsilon^2 J_{1-}^2 - \epsilon J_{2+}^2 - \epsilon^2 J_{2-}^2 - \epsilon J_{3+}^2 - \epsilon^2 J_{3-}^2 + \epsilon J_{4+}^2 + \epsilon^2 J_{4-}^2 && (4.16)\\
Q_{T_{23}^y} &= \epsilon^2 J_{1+}^2 + \epsilon J_{1-}^2 - \epsilon^2 J_{2+}^2 - \epsilon J_{2-}^2 + \epsilon^2 J_{3+}^2 + \epsilon J_{3-}^2 - \epsilon^2 J_{4+}^2 + \epsilon J_{4-}^2 && (4.17)\\
Q_{T_{23}^z} &= J_{1+}^2 + J_{1-}^2 + J_{2+}^2 + J_{2-}^2 - J_{3+}^2 - J_{3-}^2 + J_{4+}^2 - J_{4-}^2 && (4.18)\\
Q_{T_{12}^x} &= i\epsilon J_{1+}^2 - \epsilon^2 J_{1-}^2 - \epsilon J_{2+}^2 + \epsilon^2 J_{2-}^2 - \epsilon J_{3+}^2 + \epsilon^2 J_{3-}^2 + \epsilon J_{4+}^2 - \epsilon^2 J_{4-}^2) && (4.19)
\end{aligned}
$$

$$
\begin{aligned}
Q_{T^y_{12}} &= i(\epsilon^2 J^2_{1+} - \epsilon J^2_{1-} - \epsilon^2 J^2_{2+} + \epsilon J^2_{2-} + \epsilon^2 J^2_{3+} - \epsilon J^2_{3-} - \epsilon^2 J^2_{4+} + \epsilon J^2_{4-}) && (4.20)\\
Q_{T^z_{12}} &= i(J^2_{1+} - J^2_{1-} + J^2_{2+} - J^2_{2-} + J^2_{3+} - J^2_{3-} + J^2_{4+} - J^2_{4-}) && (4.21)\\
Q_{A12} &= (\{J_{1+}, J_{1-}\} + \{J_{2+}, J_{2-}\} + \{J_{3+}, J_{4-}\} + \{J_{4+}, J_{4-}\})/2 && (4.22)\\
Q_{T^x_{24}} &= (\{J_{1+}, J_{1-}\} - \{J_{2+}, J_{2-}\} - \{J_{3+}, J_{4-}\} + \{J_{4+}, J_{4-}\})/2 && (4.23)\\
Q_{T^y_{24}} &= (\{J_{1+}, J_{1-}\} - \{J_{2+}, J_{2-}\} + \{J_{3+}, J_{4-}\} - \{J_{4+}, J_{4-}\})/2 && (4.24)\\
Q_{T^z_{24}} &= (\{J_{1+}, J_{1-}\} + \{J_{2+}, J_{2-}\} - \{J_{3+}, J_{4-}\} - \{J_{4+}, J_{4-}\})/2 && (4.25)
\end{aligned}
$$

Here $\{A, B\} = AB + BA$ is the anticommutator. Note that $J_x = \frac{J_+ + J_-}{2}$ and $J_y = \frac{J_+ - J_-}{2i}$. We use these relations to calculate the Steven equivalent operators in terms of quadrupole operators. Using Wolfram's Mathematica to aid in simplifying our expressions, we found

$$
\begin{aligned}
O^0_2 &= 2Q_{A_{11}} - Q_{A_{12}} && (4.26)\\
O^0_4 &= 19Q_{A_{11}} - 6Q_{A_{12}} + 2Q^2_{A_{11}} - 6Q_{A_{11}}Q_{A_{12}} + \frac{3}{4}Q^2_{A_{12}} + 2\vec{Q}^2_{T_{21}}\\
&\quad -6\vec{Q}_{T_{21}} \cdot \vec{Q}_{T_{24}} + \frac{3}{4}\vec{Q}^2_{T_{24}} && (4.27)\\
O^0_6 &= 234Q_{A_{11}} - 60Q_{A_{12}} + \frac{125}{2}Q^2_{A_{11}} - \frac{445}{4}Q_{A_{11}}Q_{A_{12}} + 10Q^2_{A_{12}} - \frac{125}{2}\vec{Q}^2_{T_{21}}\\
&\quad -\frac{445}{4}\vec{Q}_{T_{21}} \cdot \vec{Q}_{T_{24}} + 10\vec{Q}^2_{T_{24}} + Q^3_{A_{11}} - \frac{15}{2}Q^2_{A_{11}}Q_{A_{12}} + \frac{45}{8}Q_{A_{11}}Q^2_{A_{12}} - \frac{5}{16}Q^3_{A_{12}}\\
&\quad +Q_{A_{11}}\vec{Q}^2_{T_{21}} - 15Q_{A_{11}}\vec{Q}_{T_{21}} \cdot \vec{Q}_{T_{24}} + \frac{45}{8}Q_{A_{11}}\vec{Q}^2_{T_{24}} - \frac{15}{2}Q_{A_{12}}\vec{Q}^2_{T_{21}} + \frac{45}{4}Q_{A_{12}}\vec{Q}_{T_{21}} \cdot \vec{Q}_{T_{24}}\\
&\quad +\frac{15}{16}Q_{A_{12}}\vec{Q}^2_{T_{24}} + Q^3_{T_{21}} - \frac{15}{2}Q^2_{T_{21}}Q_{T_{24}} + \frac{45}{8}Q^2_{T_{24}}Q_{T_{21}} - \frac{5}{16}Q^3_{T_{24}} && (4.28)\\
O^3_4 &= \frac{1}{8}Q_{E_1}Q_{E_2} + \frac{1}{8}\vec{Q}_{T_{11}} \cdot \vec{Q}_{T_{12}} + \frac{1}{8}\vec{Q}_{T_{22}} \cdot \vec{Q}_{T_{23}} && (4.29)
\end{aligned}
$$

$$
\begin{aligned}
O_6^3 &= -\frac{59}{8}Q_{E_1}Q_{E_2} - \frac{59}{8}\vec{Q}_{T_{11}}\cdot\vec{Q}_{T_{12}} + \frac{1}{4}Q_{A_{11}}Q_{E_1}Q_{E_2} - \frac{59}{8}\vec{Q}_{T_{22}}\cdot\vec{Q}_{T_{23}} + \frac{1}{4}Q_{A_{11}}\vec{Q}_{T_{11}}\cdot\vec{Q}_{T_{12}} \\
&\quad -\frac{1}{4}Q_{Q_{11}}\vec{Q}_{T_{22}}\cdot\vec{Q}_{T_{23}} - \frac{3}{32}Q_{A_{12}}Q_{E_1}Q_{E_2} - \frac{3}{32}Q_{A_{12}}\vec{Q}_{T_{11}}\cdot\vec{Q}_{T_{12}} - \frac{3}{32}Q_{A_{12}}\vec{Q}_{T_{22}}\cdot\vec{Q}_{T_{23}} \\
&\quad -\frac{1}{4}Q_{Q_{11}}\vec{Q}_{T_{22}}\cdot\vec{Q}_{T_{23}} - \frac{3}{32}Q_{A_{12}}Q_{E_1}Q_{E_2} - \frac{3}{32}Q_{A_{12}}\vec{Q}_{T_{11}}\cdot\vec{Q}_{T_{12}} - \frac{3}{32}Q_{A_{12}}\vec{Q}_{T_{22}}\cdot\vec{Q}_{T_{23}} \\
&\quad +\frac{1}{8}Q_{E_1}Q_{T_{12}}Q_{T_{21}} - \frac{3}{64}Q_{E_1}Q_{T_{12}}Q_{T_{24}} + \frac{1}{4}Q_{E_1}Q_{T_{21}}Q_{T_{22}} \\
&\quad -\frac{3}{64}Q_{E_1}Q_{T_{23}}Q_{T_{24}} + \frac{1}{4}Q_{E_2}Q_{T_{11}}Q_{T_{21}} \qquad (4.30)
\end{aligned}
$$

$$
\begin{aligned}
O_6^6 &= \frac{1}{32}Q_{E_2}^3 - \frac{3}{256}Q_{E_2}Q_{T_12}^2 - \frac{3}{64}Q_{E_-}Q_{T_{12}}Q_{T_{23}} + \frac{3}{128}Q_{E_2}Q_{T_23}^2 - \frac{3}{128}Q_{T_{12}}^2Q_{T_{23}} \\
&\quad +\frac{1}{128}Q_{T_{23}}^3 \qquad (4.31)
\end{aligned}
$$

where

$$
\begin{aligned}
Q_{T_2}^3 &= 6Q_{T_{2x}}Q_{T_{2y}}Q_{T_{2z}} && (4.32)\\
Q_{T_{2i}}^2Q_{T_{2j}} &= 2Q_{T_{2ix}}Q_{T_{2iy}}Q_{T_{2jz}} + Q_{T_{2ix}}Q_{T_{2iz}}Q_{T_{2jy}} + Q_{T_{2iz}}Q_{T_{2iy}}Q_{T_{2jx}} && (4.33)\\
Q_{E_i}Q_{E_j} &= Q_{E_{i+}}Q_{E_{j-}} + Q_{E_{i-}}Q_{E_{j+}} && (4.34)\\
Q_E^3 &= Q_{E_+}^3 + Q_{E_-}^3 && (4.35)\\
Q_EQ_T^2 &= 2((\varepsilon Q_{E_+} + \varepsilon^2Q_{E_-})Q_{T_x}^2 + (\varepsilon^2Q_{E_+} + \varepsilon Q_{E_-})Q_{T_y}^2 \\
&\quad +(Q_{E_+} + Q_{E_-})Q_{T_z}^2 && (4.36)\\
Q_EQ_{T_1}Q_{T_2} &= i((\varepsilon Q_{E_+} - \varepsilon^2Q_{E_-})Q_{T_{1x}}Q_{T_{2x}} + (\varepsilon^2Q_{E_+} - \varepsilon Q_{E_-})Q_{T_{1y}}Q_{T_{2y}} + \\
&\quad (Q_{E_+} - Q_{E_-})Q_{T_{1z}}Q_{T_{2z}}) && (4.37)\\
Q_EQ_{T_{2i}}Q_{T_{2j}} &= (\varepsilon Q_{E_+} + \varepsilon^2Q_{E_-})Q_{T_{2ix}}Q_{T_{2jx}} + (\varepsilon^2Q_{E_+} + \varepsilon Q_{E_-})Q_{T_{2iy}}Q_{T_{2jy}} \\
&\quad +(Q_{E_+} + Q_{E_-})Q_{T_{2iz}}Q_{T_{2jz}} && (4.38)
\end{aligned}
$$

$$
\begin{aligned}
Q_{T_{1i}}Q_{T_{1j}}Q_{T_2} &= (Q_{T_{1iz}}Q_{T_{1jy}} + Q_{T_{1iy}}Q_{T_{1jz}})Q_{T_{2x}} + (Q_{T_{1iz}}Q_{T_{1jx}} + Q_{T_{1ix}}Q_{T_{1jz}})Q_{T_{2y}} \\
&\quad +(Q_{T_{1ix}}Q_{T_{1jy}} + Q_{T_{1iy}}Q_{T_{1jx}})Q_{T_{2z}} \qquad (4.39) \\
Q_{T_1}Q_{T_{2i}}Q_{T_{2j}} &= Q_{T_{1x}}(Q_{T_{2iy}}Q_{T_{2jz}} - Q_{T_{2iz}}Q_{T_{2jy}} + Q_{T_{1y}}(Q_{T_{2iz}}Q_{T_{2jx}} - Q_{T_{2ix}}Q_{T_{2jz}}) \\
&\quad +Q_{T_{1z}}(Q_{T_{2ix}}Q_{T_{2jy}} - Q_{T_{2iy}}Q_{T_{2jx}}) \qquad (4.40) \\
Q_{T_{2i}}Q_{T_{2j}}Q_{T_{2k}} &= Q_{T_{2iz}}Q_{T_{2jy}} + Q_{T_{2iy}}Q_{T_{2jz}})Q_{T_{2kx}} + (Q_{T_{2iz}}Q_{T_{2jx}} + Q_{T_{2ix}}Q_{T_{1jz}})Q_{T_{2ky}} \\
&\quad +(Q_{T_{2ix}}Q_{T_{2jy}} + Q_{T_{2iy}}Q_{T_{1jx}})Q_{T_{2kz}} \qquad (4.41)
\end{aligned}
$$

4.3 Crystal electric field Hamiltonian (H_{CEF}) calculation

We substituted the Steven equivalent operators into H_{CEF} (2.37) to find H_{CEF} expressed in terms of the quadrapole operators. The constants B_n^m for $Tb_2Ti_2O_7$ (2.38-2.43) and $Er_2Ti_2O_7$ (2.44-2.49) were used to calculate numerical coefficients for the quadrapole terms in H_{CEF}. For example, from equations (2.31-2.36) and (2.37), the coefficient before Q_{A11} should be

$$2B_0^0 + 19B_4^0 + 234B_6^0 \qquad (4.42)$$

By using the value of the constants that are shown in equations (2.38 -2.43), the coefficient will be

$$2(-0.34) + 19(4,9 \times 10^{-3}) + 234(-7.9 \times 10^{-6}) = 0.58 \text{ meV} = 6.7 \text{ K}. \qquad (4.43)$$

We used Wolfram's Mathematica to calculate the rest of the coefficients of the quadrapole operators in H_{CEF} for $Tb_2Ti_2O_7$ and $Er_2Ti_2O_7$. The results are given in Table 4.1. They are different because each material has a different constants in H_{CEF}.

4.4 Discussion

We examine the quadratic terms in H_{CEF} as shown in Table 4.1 to look for instabilities in quadrupolar order parameters as a possible origin of elastic softening in $Tb_2Ti_2O_7$. We note that Table 4.1 contains at least two different quadrupole operators associated with each irreducible representation Q_{A_1}, Q_E, Q_{T_1}, Q_{T_2}. These are indexed by a second subscript. The second order in Q terms all appear in the combinations $a_i^2 Q_i^2 + a_j^2 Q_j^2 + a_{ij} Q_i Q_j$. These forms can be separated by taking linear combinations of Q_i and Q_j. For example, for $Tb_2Ti_2O_7$, we have (according to Table 4.1), $0.107 Q_{A_{11}}^2 - 0.327 Q_{A_{11}} Q_{A_{12}} + 0.4129 Q_{A_{12}}^2$. This can be re-written as $0.24 Q_{A_{11}}'^2 - 0.093 Q_{A_{12}}'^2$, where $Q'_{A_{11}} = 0.77 Q_{A_{11}} - 0.63 Q_{A_{12}}$ and $Q'_{A_{12}} = -0.63 Q_{A_{11}} - 0.77 Q_{A_{12}}$. Because of the negative coefficient for $Q_{A_{12}}'^2$, we identify $Q'_{A_{12}}$ as the unstable order parameter. After separating all of the terms in this way, we find that the coefficients of the quadratic terms in Q_{A_1}, Q_E and Q_{T_2} are the exactly the same. We also find that magnitudes of the coefficients are greater for $Tb_2Ti_2O_7$ than for $Er_2Ti_2O_7$. The significance of this remains an open question.

The elastic constants are sensitive to phase transitions in a system. Phase transitions involving order parameters with the same symmetry as the elastic strains can cause the elastic constants to soften far above the transition temperature. This behaviour is observed in $Tb_2Ti_2O_7$, where the transition temperature is unknown because it is below any accessible temperature. The order parameter of that transition is also unknown. One possibility is that it is quadrupolar ordering of f-electrons in the system. In this chapter we have investigated the possibility that the order parameter is a quadrupolar OP whose instability originates in the crystal electric field Hamiltonian.

In Landau theory, a phase transition occurs when the coefficient of the quadratic term in an order parameter in the free energy becomes less than zero. So we are

Quadrupole operator	$Tb_2Ti_2O_7$	$Er_2Ti_2O_7$
$Q_{A_{11}}$	-6.76	2.08
$Q_{A_{12}}$	3.57	-0.977
$Q^2_{A_{11}}$	0.107	0.0409
$Q_{A_{11}}Q_{A_{12}}$	-0.327	-0.113
$Q^2_{A_{12}}$	0.04129	0.01362
$Q_{E_1}Q_{E_2}$	0.0513	0.0337
$\vec{Q}_{T_{11}} \cdot \vec{Q}_{T_{12}}$	0.0512	0.0337
$\vec{Q}^2_{T_{21}}$	0.1068	0.0409
$\vec{Q}_{T_{21}} \cdot \vec{Q}_{T_{24}}$	-0.327	-0.113
$Q^3_{A_{11}}$	-0.0000918	0.000126
$Q^2_{A_{11}}Q_{A_{12}}$	0.000689	0.000949
$Q_{A_{11}}Q^2_{A_{12}}$	-0.000516	0.00071
$Q^3_{A_{12}}$	0.0000287	0.0000395
$Q_{A_{11}}Q_{E_1}Q_{E_2}$	0.0003788	-0.000522
$Q_{A_{12}}Q_{E_1}Q_{E_2}$	-0.000142	0.000196
$Q_{A_{11}}\vec{Q}_{T_{11}} \cdot \vec{Q}_{T_{12}}$	0.000379	-0.000522

Table 4.1: The coefficients of quadrupole operators of the crystal electric field Hamiltonian (in kelvin).

seeking a free energy with that property. We assumed that a free energy could be derived from a Hamiltonian, where to a first approximation the order parameter is the expectation value of the quantum mechanical operators, and so the quadratic terms in H_{CEF} are related to the quadratic terms in the free energy. The derivation of higher order terms in the free energy is an extremely difficult problem, not attempted in this thesis.

We conclude that the crystal electric field Hamiltonian may be the origin of the elastic softening in $Tb_2Ti_2O_7$.

Quadrupole operator	$Tb_2Ti_2O_7$	$Er_2Ti_2O_7$
$Q_{A_{11}}\vec{Q}^2_{T_{21}}$	-0.000275	0.000379
$Q_{A_{11}}\vec{Q}_{T_{21}}\cdot\vec{Q}_{T_{24}}$	0.00138	-0.00189
$Q_{A_{11}}\vec{Q}_{T_{22}}\cdot\vec{Q}_{T_{23}}$	0.000379	- 0.000522
$Q_{A_{11}}\vec{Q}^2_{T_{24}}$	-0.000516	0.000711
$Q_{A_{12}}\vec{Q}_{T_{11}}\cdot\vec{Q}_{T_{12}}$	-0.000142	0.000196
$Q_{A_{12}}\vec{Q}^2_{T_{21}}$	0.000688	0.000949
$Q_{A_{12}}\vec{Q}_{T_{21}}\cdot\vec{Q}_{T_{24}}$	-0.00103	0.00142
$Q^3_{E_2}$	-0.000389	0.0000543
$Q_{E_1}Q_{T_{12}}Q_{T_{21}}$	0.000189	0.000261
$Q_{E_1}Q_{T_{12}}Q_{T_{24}}$	0.000071	0.000098
$Q_{A_{12}}\vec{Q}_{T_{22}}\cdot\vec{Q}_{T_{23}}$	-0.000142	0.000196
$Q_{A_{12}}\vec{Q}^2_{T_{24}}$	0.00008607	-0.0001185
$\vec{Q}_{T_{22}}\cdot\vec{Q}_{T_{23}}$	0.0512	0.0337
$\vec{Q}^2_{T_{24}}$	0.0413	0.0136
$Q_{E_1}Q_{T_{21}}Q_{T_{23}}$	0.000189	-0.000261
$Q_{E_1}Q_{T_{23}}Q_{T_{24}}$	-0.000071	0.0000979
$Q_{E_2}Q^2_{T_{12}}/2$	0.00002924	-0.0000408
$Q_{E_2}Q_{T_{11}}Q_{T_{21}}$	0.000379	0.000522
$Q_{E_2}Q_{T_{11}}Q_{T_{24}}$	0.000142	0.000196
$Q_{E_2}Q_{T_{12}}Q_{T_{23}}$	0.0000584	0.0000815
$Q_{E_2}Q_{T_{21}}Q_{T_{22}}$	0.000379	-0.000522
$Q_{T_{11}}Q_{T_{12}}Q_{T_{21}}$	-0.000189	0.000261
$Q_{T_{11}}Q_{T_{12}}Q_{T_{24}}$	0.000071	0.000098
$Q_{T_{11}}Q_{T_{21}}Q_{T_{23}}$	0.000328	0.000452
$Q_{T_{11}}Q_{T_{23}}Q_{T_{24}}$	-0.000123	0.000169
$Q_{T_{12}}Q_{T_{21}}Q_{T_{22}}$	0.000328	0.000452
$Q_{T_{12}}Q_{T_{22}}Q_{T_{24}}$	-0.000123	0.000169
$Q_{E_2}Q_{T_{22}}Q_{T_{24}}$	0.000142	-0.000195

Quadrupole operator	$Tb_2Ti_2O_7$	$Er_2Ti_2O_7$
$Q^2_{T_{12}}Q_{T_{23}}/2$	0.0000584	-0.0000816
$Q^3_{T_{21}}/6$	-0.000551	0.000758
$Q^2_{T_{21}}Q_{T_{24}}/2$	0.00138	0.000196
$Q_{T_{21}}Q_{T_{22}}Q_{T_{23}}$	-0.000189	0.000261
$Q_{T_{21}}Q^2_{T_{24}}/2$	-0.00103	0.00142
$Q_{22}Q_{T_{23}}Q_{T_{24}}$	0.000071	-0.0000979
$Q^3_{T_{23}}/6$	0.0000585	0.0000816
$Q^3_{T_{24}}/6$	0.000172	-0.000237
$Q^2_{T_{12}}Q_{T_{23}}/2$	0.0000584	-0.0000816
$Q^3_{T_{21}}/6$	-0.000551	0.000758
$Q^2_{T_{21}}Q_{T_{24}}/2$	0.00138	0.000196
$Q_{T_{21}}Q_{T_{22}}Q_{T_{23}}$	-0.000189	0.000261
$Q_{T_{21}}Q^2_{T_{24}}/2$	-0.00103	0.00142
$Q_{22}Q_{T_{23}}Q_{T_{24}}$	0.000071	-0.0000979
$Q^3_{T_{23}}/6$	0.0000585	0.0000816
$Q^3_{T_{24}}/6$	0.000172	-0.000237
$Q^2_{T_{12}}Q_{T_{23}}/2$	0.0000584	-0.0000816
$Q^3_{T_{21}}/6$	-0.000551	0.000758
$Q^2_{T_{21}}Q_{T_{24}}/2$	0.00138	0.000196
$Q_{T_{21}}Q_{T_{22}}Q_{T_{23}}$	-0.000189	0.000261
$Q_{T_{21}}Q^2_{T_{24}}/2$	-0.00103	0.00142
$Q_{22}Q_{T_{23}}Q_{T_{24}}$	0.000071	-0.0000979
$Q^3_{T_{23}}/6$	0.0000585	0.0000816
$Q^3_{T_{24}}/6$	0.000172	-0.000237

Chapter 5

Conclusion

5.1 Magnetic ordering in $Er_2Ti_2O_7$

The main purpose in this part of the thesis is to calculate the temperature at which the J_E order parameter becomes unstable in $Er_2Ti_2O_7$. To do this, we applied the molecular field method to successively more complicated cases. First, we found the formula for transition temperature for the 1D spin-$\frac{1}{2}$ ferromagnet. Then the transition temperature for a 1D spin-$\frac{1}{2}$ antiferromagnet was calculated using first the same procedure and then by grouping the spins. Then, we considered $Er_2Ti_2O_7$, where the four spins on the 4b Wyckoff position were considered in groups. We found the transition temperature for a J_A magnetic order parameter before tackling the more complicated J_E order parameter. We found that J_E becomes unstable at $T_N = 93K$, which marks the onset of a Goldstone mode. The magnetic phase transition occurs at a lower temperature, probably due to the order-by-disorder mechanism.

5.2 Analysis of crystal electric Hamiltonian of $Tb_2Ti_2O_7$ and $Er_2Ti_2O_7$

$Tb_2Ti_2O_7$ becomes soft at low temperatures. This softening can be accounted for by a linear coupling between the elastic strain and some type of order parameter. We investigated quadrupolar order parameters contained in crystal electric field Hamiltonian. We examined the crystal electric field Hamiltonian for $Tb_2Ti_2O_7$ by rewriting it in terms of quadrupolar operators, and comparing it to a similar calculation for $Er_2Ti_2O_7$. The calculation determined the numerical coefficients for the quadrupole terms in H_{CEF}. While H_{CEF} has instabilities in both $Er_2Ti_2O_7$ and $Tb_2Ti_2O_7$, they appear to be larger in $Tb_2Ti_2O_7$.

According to the Landau theory, when the coefficient of the quadrabic term in the order parameter in the free energy is less than zero, a phase transition occurs. We supposed that the free energy can be derived from crystal electric field Hamiltonian, and the quadratic terms in the quadrapole operators in H_{CEF} give rise to quadratic terms in the order parameter in the free energy, where the order parameter is the expectation value of the quadrupole operators. In fact, the derivation of higher order terms in the free energy will be even more complicated. Consequently, we can say in the end that the crystal electric field may contribute to the unusual elastic softening in $Tb_2Ti_2O_7$; whether or not this is the main cause remains an open question.

5.3 Future work

Future studies related to the work presented in this thesis include the following possibilities. First, it would be straightfoward to use the methods of this thesis to calculate the transition temperatures associated with the other magnetic order parameters, $\vec{J}_{T_{11}}$,

$\vec{J}_{T_{12}}$, and $\vec{J}_{T_3}$. Second, it would be interesting to compare the size fo the quadrupolar order parameter coefficients for other rare earth pyrochlores to compare with our results for $Tb_2Ti_2O_7$.

Bibliography

[1] M. J. Harris and M. P. Zinkin, *Modern Physics Letters B* **10**, 417438 (1996).

[2] S. D. Barrett, *The Structure of Rare-Earth Metal Surface* (World Scientific, 2001).

[3] A. G. Maestro and M. J. Gingras, *Journal of Physics: Condensed Matter* **16**, 33393353 (2004).

[4] C. Lacroix, P. Mendels, and F. Mila, *Introduction To Frustrated Magnetism* (Springer Series in Solid Sciences, 2011).

[5] T. Fennell, M. Kenzelmann and B. Roessli, *Physics Review Letters* **112**, 017203 (2014).

[6] M. E. Zhitomirsky, M. V. Gvozdikova, P. C. W. Holdsworth and R. Moessner, *Physical Review Letters* **109**, 077204 (2012).

[7] T. Fennell, P. P. Deen and A. R. Wildes, *Science* **326**, 415 (2009).

[8] J. S. Gardner, B. D. Gaulin, A. J. Berlinsky and P. Waldron, *Physics Review B* **64**, 224416 (2001).

[9] V. V. Klekovkina and B. Z. Malkin, *Optic and Spectroscopy* **116**, 849857 (2014).

[10] Y. Nakanishi, T. Kumagai and M. Yoshizawa, *Physical Review B* **83**, 184434 (2011).

[11] S. Han, J. S. Gardner and C. H. Booth, *Physical Review B* **69**, 024416 (2004).

[12] J. S. Gardner, S. R. Dunsiger and B. D. Gaulin, *Physical Review letters* **82**, 1012 (1999).

[13] J. S. Gardner, M. J. Gingras and J. E. Greedan, *Review of Modern Physics* **82**, 53 (2010).

[14] E. Lhotel, C. Paulsen and S. Vanishri, *Physics Review B* **86**, 020410 (2012).

[15] H. Tsunetsugu, *Physics Review B* **65**, 024415 (2001).

[16] O. A. Petrenko, M. R. Lees and G. Balakrishnan, *European Physical Journal B* **112**, 017203 (2013).

[17] P. Bonville, S. Petit and C. Paulsen, *Journal of Physics: Condensed Matter* **25**, 275601 (2013).

[18] J. D. Champion, M. J. Harris and E. Cizmar, *Physical Review B* **68**, 020401 (2003).

[19] A. P. Ramirez, A. Hayashi, R. J. Cava and R. Siddharthan, *Nature* **399**, 333335 (1999).

[20] M. J. Harris, S. T. Bramwell and K. W. Godfrey, *Physical Review Letters* **79**, 13 (1997).

[21] D. C. Marinescu, *Classical And Quantum Information* (Academic Press, 2011).

[22] C. Castelnovo, R. Moessner and S. L. Sondhi, *Nature* **451**, 06433 (2008).

[23] H. Y. Xiao and W. J. Weber, *Journal of Applied Physics* **104**, 073503(2008).

[24] K. B. Helean, S. V. Ushakov, C. E. Brown, A. Navrotsky, J. Lian, R. C. Ewing, J. M. Farmer and L. A. Boatner, *Journal of Solid State Chemistry* **177**, 1858-1866 (2004).

[25] M. Glazer and G. Burne, *Space Groups For Solid State Scientists* (Academec Press, 2013).

[26] U. Shmueli, *International Table for Crystallography* (Springer Science and Business Media, 2008).

[27] M. Tinkhan, *Group Theory and Quantum Mechanics* (Dover Publication, 2003).

[28] Jie Lian, L. M. Wang and Rodney Ewing, *Physical Review B* **68**, 134107 (2003).

[29] T. T. A.Lummen, L. P. Handayani, M .C. Donker, D. Fausti, G. Dhalenne, P. Berthet, A. Revcolenschi and P. H. M. Van Loosdrecht, *Physical Review B* **77**, 214310 (2008).

[30] M. J. P. Gingras, B. C. den Hertog, M. Faucher, J. S. Gardner, S. R. Dunsiger, L. J. Chang and B. D. Gaulin, *Physical Review Letters* **62**, 6496 (2000).

[31] John E. Greedan, *Journal of Alloys and Compounds* **37**, 37099882 (2006).

[32] A. P. Ramirez, *Annual Reviews Material Science* **24**, 453-80 (1994).

[33] S.H. Curnoe, *Physical Review B* **78**, 094418 (2008).

[34] L. Savary, K. A. Ross and B. D. Gaulin, *Physical Review Letters* **109**, 167201 (2012).

[35] P. A. Mc Clarty, S. H. Curnoe and M. J. P. Gingras, *Journal of Physics: Conference Series* **145**, 01202 (2004).

[36] S. Onada and L. Balents, *Physical Review B* **86**, 104412 (2012).

[37] S. Petit, P. Bonville, J. Robert and C. Decorse , *Physical Review B* **86**, 174403 (2012).

[38] A. Poole, A. S. Wills and E. Lelievie-Berna, *Journal of Physics: Condens Matter* **19**, 452201 (2007).

[39] A. K. R. Briffa, R. J. Mason and M. W. Long, *Physical Review B* **84**, 094427 (2011).

[40] S. Blundell, *Magnetism in Condensed Matter* (OUP Oxford, 2001).

[41] A. Szytuda, *Handbook of Crystal Structure And Magnetic Properties of Rare Earth Intermetallics* (CRC Press, 1994).

[42] A. Visintin, *Physica B: Condensed Matter* **275**, 87-91 (2000).

[43] J. M. Yeomans, *Statistical Mechanics of Phase Transition* (Oxford University Press, 1992).

[44] A. Bertin, Y. Chapuis, P. Dalmas and A. Yaouance, *Journal of Physics: Condensed Matter* **24**, 256003 (2012).

[45] J. Zhang, K. Fritsch, B. V. Bagheri and B. D. Gaulin, *Physical Review B* **89**, 134410 (2014).

[46] A. Abragan and B. Bleaney, *Electron Paramagnetic Resonance of Transition Ions* (Clarendon Press, 1970).

[47] G. M. Brun, *Physical Review A* **90**, 023621 (2014).

[48] V. V. Klekovkina and B. Z. Malkin *Journal of Physics: Conference series* **324**, 012036 (2011).